

# Journal Pre-proof

Novel cyclometalated Ru(II) complexes containing isoquinoline ligands: Synthesis, characterization, cellular uptake and *in vitro* cytotoxicity

Jincan Chen, Jie Wang, Yuanyuan Deng, Baojun Li, Chengpeng Li, Yuxue Lin, Dongbin Yang, Huanyun Zhang, Lanmei Chen, Tao Wang



PII: S0223-5234(20)30534-1

DOI: <https://doi.org/10.1016/j.ejmech.2020.112562>

Reference: EJMECH 112562

To appear in: *European Journal of Medicinal Chemistry*

Received Date: 28 April 2020

Revised Date: 29 May 2020

Accepted Date: 10 June 2020

Please cite this article as: J. Chen, J. Wang, Y. Deng, B. Li, C. Li, Y. Lin, D. Yang, H. Zhang, L. Chen, T. Wang, Novel cyclometalated Ru(II) complexes containing isoquinoline ligands: synthesis, characterization, cellular uptake and *in vitro* cytotoxicity, *European Journal of Medicinal Chemistry*, <https://doi.org/10.1016/j.ejmech.2020.112562>.

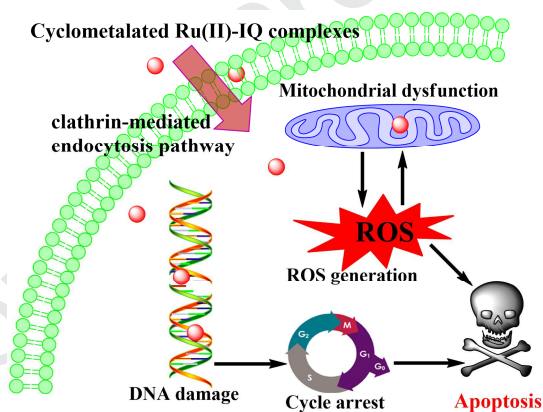
This is a PDF file of an article that has undergone enhancements after acceptance, such as the addition of a cover page and metadata, and formatting for readability, but it is not yet the definitive version of record. This version will undergo additional copyediting, typesetting and review before it is published in its final form, but we are providing this version to give early visibility of the article. Please note that, during the production process, errors may be discovered which could affect the content, and all legal disclaimers that apply to the journal pertain.

© 2020 Elsevier Masson SAS. All rights reserved.

## Graphical Abstract

**Novel cyclometalated Ru(II) complexes containing isoquinoline ligands: synthesis, characterization, cellular uptake and *in vitro* cytotoxicity**

The cellular uptake, *in vitro* cytotoxicities, *in vivo* toxicity, cell cycle arrest and apoptosis-inducing mechanism of two new cyclometalated ruthenium(II)-isoquinoline complexes have been extensively explored by ICP-MS, MTT assay, flow cytometry, zebrafish embryos model, inverted fluorescence microscope as well as western blot experimental techniques.



# Novel cyclometalated Ru(II) complexes containing isoquinoline ligands: synthesis, characterization, cellular uptake and *in vitro* cytotoxicity

Jincan Chen,<sup>a</sup> Jie Wang,<sup>a</sup> Yuanyuan Deng,<sup>a</sup> Baojun Li,<sup>a</sup> Chengpeng Li,<sup>b</sup> Yuxue Lin,<sup>a</sup>  
Dongbin Yang,<sup>c</sup> Huanyun Zhang,<sup>c</sup> Lanmei Chen,<sup>a\*</sup> Tao Wang,<sup>d,e\*</sup>

<sup>a</sup> Guangdong Key Laboratory for Research and Development of Nature Drugs, School of Pharmacy, Guangdong Medical University, Zhanjiang, 524023, China

<sup>b</sup> The Public Service Platform of South China Sea for R&D Marine Biomedicine Resources, Marine Biomedical Research Institute, Guangdong Medical University, Zhanjiang, 524023, China

<sup>c</sup> The Affiliated People's Hospital of Hebi of Henan University, Hebi, 456030, China

<sup>d</sup> The College of Nursing and Health, Zhengzhou University, Zhengzhou, 450001, China

<sup>e</sup> Centre for Comparative Genomics, Murdoch University, Perth, WA 6150, Australia

\*Corresponding author. E-mail addresses: [lanmeichen@126.com](mailto:lanmeichen@126.com) (L.M. Chen), [Tao.Wang@murdoch.edu.au](mailto:Tao.Wang@murdoch.edu.au) (T. Wang)

## Abstract

Two novel cyclometalated Ru(II) complexes containing isoquinoline ligand, [Ru(bpy)<sub>2</sub>(1-Ph-IQ)](PF<sub>6</sub>)<sub>2</sub> (bpy = 2,2'-bipyridine; 1-Ph-IQ= 1-phenylisoquinoline; **RuIQ-1**) and [Ru(phen)<sub>2</sub>(1-Ph-IQ)](PF<sub>6</sub>)<sub>2</sub> (phen = 1,10-phenanthroline; **RuIQ-2**) were found to show high cytotoxic activity against NCI-H460, A549, HeLa and MCF-7 cell lines. Notably, both of them exhibited IC<sub>50</sub> values that were an order of magnitude lower than those of clinical cisplatin and two structurally similar Ru(II)-isoquinoline complexes [Ru(bpy)<sub>2</sub>(1-Py-IQ)](PF<sub>6</sub>)<sub>2</sub> (**Ru3**) and [Ru(phen)<sub>2</sub>(1-Py-IQ)](PF<sub>6</sub>)<sub>2</sub> (**Ru4**) (1-Py-IQ=1-pyridine-2-yl). The cellular uptake and intracellular localization displayed that the two cyclometalated Ru(II) complexes entered NCI-H460 cancer cells dominantly via endocytosis pathway, and preferentially distributed in the nucleus.

Further investigations on the apoptosis-inducing mechanisms of **RuIQ-1** and **RuIQ-2** revealed that the two complexes could cause S, G2/M double-cycle arrest by regulating cell cycle related proteins. The two complexes also could reduce the mitochondrial membrane potential (MMP), promote the generation of intracellular ROS and trigger DNA damage, and then lead to apoptosis-mediated cell death. More importantly, **RuIQ-2** exhibits low toxicity both towards normal HBE cells *in vitro* and zebrafish embryos *in vivo*. Accordingly, the developed complexes hold great potential to be developed as novel therapeutics for effective and low-toxic cancer treatment.

**Keywords:** Cyclometalated Ru(II) complexes, Isoquinoline, Apoptosis, DNA damage, Low toxicity

## 1. Introduction

In recent years, transition-metal complexes have gradually found their way in various biomedical applications, ranging from antiangiogenic [1], antihypertension [2], antibacterial [3], anti-inflammation [4], antimalarial [5], to anticancer [6-11]. Over the past decades, platinum-based metal complexes have been intensively exploited in the oncological field, given the successful introduction of cisplatin in the early 1980s [12, 13]. However, the clinical application of such platinum-based metal complex has been heavily limited by issues including poor solubility, severe toxicity, and drug resistance [14, 15]. To circumvent these problems, considerable efforts have been made for the development of alternative metal-based compounds. Among the various alternative transition metals, organometallic ruthenium, featured by predictable geometry, variable oxidation states and low toxicity to normal cells [16-18], has been particularly emphasized.

By far, three Ru(III) drugs, namely NAMI-A [19], KP1019 [20], KP1339 [21], and the Ru(II)-based therapeutic, TLD1433 [22], have progressed to different stages in clinical trials. Although the further clinical investigations of NAMI-A [23] and

KP1019 [20] have been limited by low therapeutic efficiency and poor water solubility, respectively, with improved solubility and promising anticancer efficacy, KP1339 is currently undergoing clinical trials [21,24]. TLD1433, the first Ru(II)-based photosensitizer for PDT treatment of bladder cancer, recently entered phase IB clinical trials [22, 24]. However, the mechanism of action of these Ru-based drugs has not been fully understood yet.

Recently, the cyclometalated Ru(II) complexes, as a new type of non-platinum metal-based compounds, have attracted worldwide attention due to their strong safety profiles and potential anti-cancer effects, with many of them displayed different mechanisms of cytotoxic action compared with the classical cisplatin [25-28]. The cyclometalated Ru(II) compounds, in which one or more of the nitrogen donors of compounds are replaced by carbon donor atoms, are relatively stable in structure since the bond distances of Ru-C are shorter than that of Ru-N bond [29, 30]. Also, it has been shown that the cyclometalation of Ru(II) compounds formed by substituting Ru-N with Ru-C bond can improve the liposolubility of these compounds and result in increased cellular uptake of tumour tissues, an essential factor for high-efficient anti-cancer effect [27, 31, 32].

The development of Ru(II)-polypyridyl complexes with bioactive alkaloids as ligands provides a new strategy for designing novel metal-based antitumor drugs with improved activity [33-35]. Isoquinoline (IQ) and its derivatives are a class of nitrogen heterocyclic alkaloids widely existing in nature and possessing a variety of important biological functions, such as anticancer, analgesic, and anti-inflammatory effects [36]. It has been reported that isoquinoline alkaloids could inhibit the proliferation, migration and invasion of tumour cells through multiple pathways, including cycle arrest, apoptosis, inhibiting the activity of cyclooxygenase-2 (COX-2), topoisomerase and angiogenesis, etc. [37]. Also, according to the recent study performed by Liang et al., the biological activity of the isoquinoline alkaloids could be further improved via coordination of isoquinoline derivatives with metals such as  $Zn^{2+}$ ,  $Ni^{2+}$ ,  $Cu^{2+}$  [38]. The implication of these is that designing Ru(II) based cyclometalated isoquinoline

compounds, via employing synthetic diversity of the Ru(II) complexes, represents an appealing strategy for new anticancer drug development.

Based on this hypothesis, in this work, with 1-phenylisoquinoline as a ligand, two new cyclometalated Ru(II) complexes  $[\text{Ru}(\text{bpy})_2(1\text{-Ph-IQ})]^+$  (**RuIQ-1**) and  $[\text{Ru}(\text{phen})_2(1\text{-Ph-IQ})]^+$  (**RuIQ-2**) (1-Ph-IQ = 1-phenylisoquinoline) (Fig. 1) were designed and synthesized. As experimental controls, the non-cyclometalated ruthenium(II) isoquinoline complexes  $[\text{Ru}(\text{bpy})_2(1\text{-Py-IQ})](\text{PF}_6)_2$  (**Ru3**) and  $[\text{Ru}(\text{phen})_2(1\text{-Py-IQ})](\text{PF}_6)_2$  (**Ru4**) (1-Py-IQ=1-pyridine-2-yl), with a similar structure to **RuIQ-1** and **RuIQ-2**, were also prepared and characterized, and the corresponding cytotoxicity of **Ru3** and **Ru4** was explored as well. Further mechanism studies showed that the cyclometalated Ru(II) complexes, especially complex **RuIQ-2**, could effectively constrain the viability of the NCI-H460 cells through inducing S, G2/M double-cycle arrest, DNA damage, the generation of the reactive oxygen species (ROS) and ROS-mediated mitochondrial dysfunction. In addition, when the toxicity of complex **RuIQ-2** to zebrafish embryos was investigated, it was confirmed that the cyclometalated Ru(II) complexes containing isoquinoline ligands possessed superior safety profiles and therefore held great potential to be further developed as a novel chemotherapeutic agent for effective lung cancer treatment.

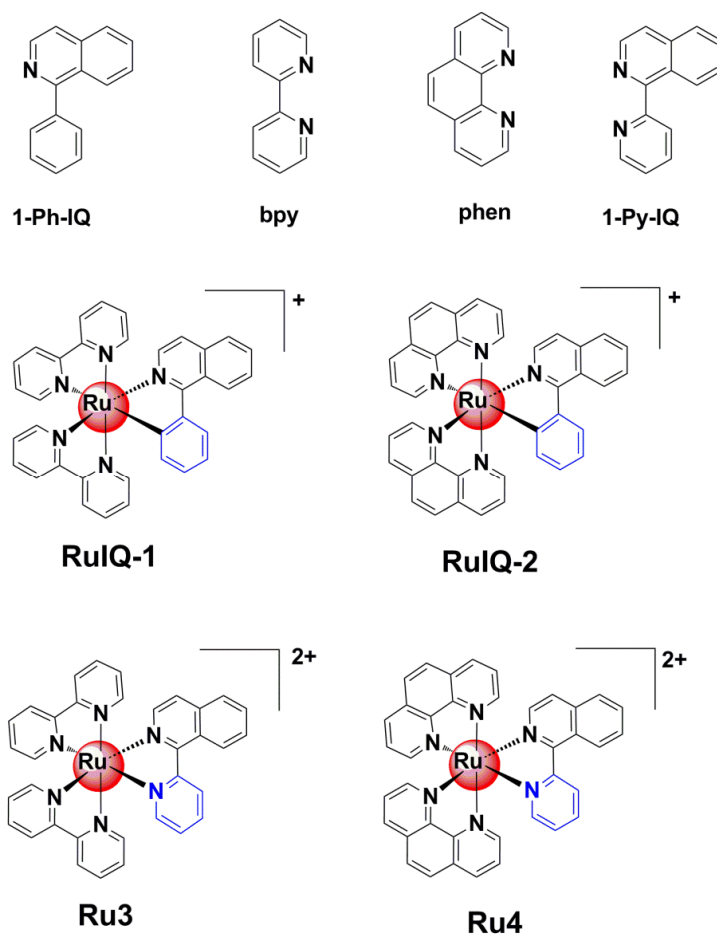


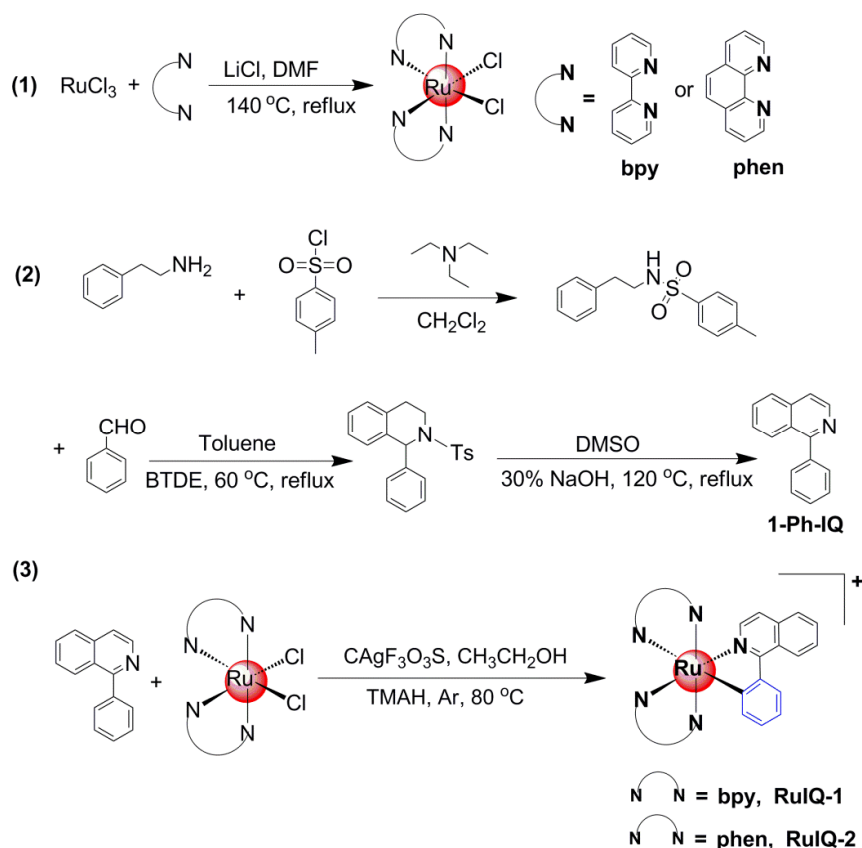
**Fig. 1.** The chemical structure of Ru(II) complexes **RuIQ-1**, **RuIQ-2**, **Ru3**, **Ru4** and their ligands.

## 2. Results and discussion

### 2.1. Synthesis, characterization and UV-visible spectral studies

The synthetic routes of precursors  $cis$ -[Ru(L)<sub>2</sub>Cl<sub>2</sub>] (L=bpy, phen), ligand 1-Ph-IQ and the cyclometalated Ru(II) complexes **RuIQ-1**, **RuIQ-2** are described in Scheme 1. Firstly, the ligand 1-Ph-IQ was synthesized according to the previously reported method [39]. Secondly, based on the reports [40, 41], refluxing RuCl<sub>3</sub>·nH<sub>2</sub>O, LiCl and bpy or phen in a solution of N,N-Dimethylformamide (DMF) at 140 °C overnight, and the precursors  $cis$ -[Ru(L)<sub>2</sub>Cl<sub>2</sub>]·2H<sub>2</sub>O (L=bpy, phen) were obtained. Finally, complexes **RuIQ-1** and **RuIQ-2** were obtained by reacting  $cis$ -[Ru(L)<sub>2</sub>Cl<sub>2</sub>] (L = bpy, phen) with 1-Ph-IQ in ethyl alcohol at 80 °C overnight under the protection of argon. Ru(II) isoquinoline complexes **Ru3** and **Ru4** were synthesized and obtained

according to previously reported methods [42, 43]. Then, complexes **RuIQ-1**, **RuIQ-2**, **Ru3**, **Ru4** were characterized by elemental analysis, ESI-MS (Fig. S1-S4 in supplementary materials),  $^1\text{H}$  NMR (Fig.S5-S8). The counter anion of all these complexes is  $\text{PF}_6^-$ .



**Scheme 1.** The synthetic route of precursors *cis*-[Ru(bpy)<sub>2</sub>Cl<sub>2</sub>], *cis*-[Ru(phen)<sub>2</sub>Cl<sub>2</sub>], ligand 1-Ph-IQ and **RuIQ-1**, **RuIQ-2**.

The UV/Vis absorption spectra of **RuIQ-1** and **RuIQ-2** in phosphate buffered saline (PBS), saline solution (NaCl), ethanol (C<sub>2</sub>H<sub>5</sub>OH), and methyl cyanide (CH<sub>3</sub>CN) at 298 K are displayed in Fig. 2. As shown in Fig. 2, **RuIQ-1** and **RuIQ-2** showed intense absorption bands that in the range of 250-300 nm, which were attributed mainly to intra-ligand  $\pi\text{-}\pi^*$  transitions [42, 44, 45]. Differing from **RuIQ-1**, the maximum absorption peak of **RuIQ-2** was correspondingly blue-shifted from 270 nm to 266 nm, the reason probably lies in the fact that the ancillary ligand phen in **RuIQ-2** has better  $\pi\text{-}\pi$  conjugated system. Besides, the relatively weak bands at the range of 300–380 nm are most likely attributed to  $\pi\text{-}\pi^*$  transitions, the relatively

broad and weak absorption at 470-570 nm are contributed by the metal-to-ligand charge transfer (MLCT) absorption.

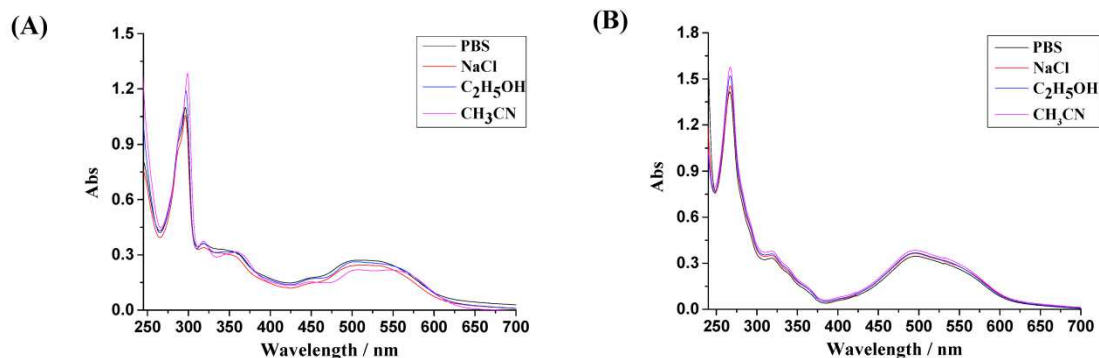


**Fig. 2.** UV-Vis spectra of Ru(II) complexes in different solvents at 298 K. (A) **RuIQ-1** (20  $\mu$ M). (B) **RuIQ-2** (20  $\mu$ M).

## 2.2. Properties of the cyclometalated Ru(II) complexes in solution

The stability of drugs plays a vital role in cellular internalization and target binding. Thus, we analyzed the aqueous stability of **RuIQ-1** and **RuIQ-2** by UV/Vis absorption spectroscopy and  $^1\text{H}$  NMR. First of all, we observed that there was no apparent change in the UV-Vis absorption of Ru(II) complexes in different solvents (PBS, saline solution,  $\text{C}_2\text{H}_5\text{OH}$ , and  $\text{CH}_3\text{CN}$ ) at 298 K (Fig. 2A and 2B). Then, we analyzed the time-dependent absorption spectra of **RuIQ-1** and **RuIQ-2** in PBS at 298 K (Fig. S9). Similarly, the absorption spectra of **RuIQ-1** and **RuIQ-2** did not change significantly within 12 h. Finally, long-term stability monitoring was assessed by  $^1\text{H}$  NMR to simulate the physiological conditions. As demonstrated in Fig. S10 and Fig. S11, after one week incubating **RuIQ-1** and **RuIQ-2** in  $\text{DMSO-}d_6/\text{D}_2\text{O}$  ( $v/v = 3:1$ ), the  $^1\text{H}$  NMR spectra did not show any significant changes compared with the original samples.

It must be noted that the Ru(II) complexes may precipitate or bind with certain biological molecules such as various plasma proteins after systematic administration, which prevents them from reaching biological targets with high concentration. To test the potential binding of Ru (II) complexes to such internal molecules, the absorption spectra of **RuIQ-1** and **RuIQ-2** incubated in aqueous solutions containing bovine serum albumin (BSA) was monitored by UV-Vis spectra at 298 K. From Fig. S12A

and Fig. S12B, it was clear that there was no obvious absorbance change in UV-Vis spectra within 24 h, suggesting no prominent binding of Ru(II) complexes with plasma proteins. Besides, the ESI-MS spectra of Ru(II) complexes showed abundant peaks of molecular ions coinciding with the molecular weights of the compounds (Fig. S12C and Fig. S12D), indicating that the precipitation or forming into other compounds did not occur under the tested conditions. The results of all these suggested that **RuIQ-1** and **RuIQ-2** were quite stable in aqueous solution.

### 2.3. Cytotoxicity assay *in vitro*

After confirming the stability of the synthesized **RuIQ-1**, **RuIQ-2**, **Ru3**, **Ru4**, the *in vitro* cytotoxicity of them, together with precursors and ligand, were assessed on NCI-H460 (human lung cancer), A549 (human non-small cell lung cancer), HeLa (human cervical cancer) and MCF-7 (breast cancer) cells via 3-(4,5-dimethylthiazol-2-yl)-2,5-diphenyltetrazolium bromide (MTT) assay, with the clinical cisplatin as control. The IC<sub>50</sub> values of the tested reagents to the illustrated cancer cells were shown in Table 1. As displayed, after the treatment of test cancer cells for 48 h, the IC<sub>50</sub> values of the ligand 1-Ph-IQ, precursors *cis*-[Ru(L)<sub>2</sub>Cl<sub>2</sub>] (L=bpy, phen) recorded a high value (approached or exceeded 200 μM) against all the tested cancer cells, and thus deemed as inactive. On the other hand, while complexes **Ru3** and **Ru4** showed moderate activity towards the tested cancer cells (with IC<sub>50</sub> values ranging from 69.1 to 88.7 μM), the new cyclometalated complexes **RuIQ-1** and **RuIQ-2** displayed higher cytotoxicity effects toward all the test cancer cells, with IC<sub>50</sub> values ranging from 1.8 to 7.2 μM. As observed on the human lung cancer NCI-H460 cells, **RuIQ-1** and **RuIQ-2** showed IC<sub>50</sub> values (2.1 μM and 1.8 μM, respectively) that are over 32- and 38-fold lower than that of **Ru3** (69.1 μM), and over 36- and 43-fold lower than that of complex **Ru4** (77.6 μM). Moreover, the activities of **RuIQ-1** and **RuIQ-2** were about 12-fold and 14-fold higher than that of the clinical cisplatin against NCI-H460 cells. Further investigation illustrated that **RuIQ-1** and **RuIQ-2** inhibited the viability of NCI-H460 cells in a time- and

concentration-dependent manner (Fig.S13). Therefore, our results provided substantial evidence that the integration of the ligand 1-Ph-IQ to organometallic Ru(II) center represents a rational strategy for the development of novel chemical compounds with enhanced anti-cancer effects.

To evaluate the potential side effects, additional cytotoxicity tests were conducted using complexes **RuIQ-1**, **RuIQ-2**, **Ru3**, **Ru4** to against the normal HBE (human bronchial epithelial) cells (Table 1). Compared with **Ru3**, **Ru4** and cisplatin control, which displayed comparable toxicity to cancer cells and normal HBE cells, complexes **RuIQ-1** and **RuIQ-2** exhibited much lower toxicity to the normal HBE cells. These results suggested that **RuIQ-1** and **RuIQ-2** possess a preferable therapeutic profile against cancer, especially lung cancer cells. This observation was further supported by the selectivity index (SI) assay (Table 1), where a clear trend was recorded as **RuIQ-2** (11.1) > **RuIQ-1** (10.5) > **Ru3** (1.4) > **Ru4** (1.3) > cisplatin (0.6). Hence, **RuIQ-2** demonstrated the highest safety profile for potential efficient cancer treatment. The above analysis also confirms that *in vitro* cytotoxicity of complexes **RuIQ-1** and **RuIQ-2** agrees with those of other cyclometalated Ru(II) complexes [26, 42]. This may attribute to the high hydrophobicity and cellular uptake caused by the unique structural characteristics of the cyclometalated ligands.

Since NCI-H460 cells were especially susceptible to **RuIQ-1** and **RuIQ-2**, with over 12- and 14-fold lower IC<sub>50</sub> values than that of cisplatin under the identical conditions, this cell line was then selected as a cell model for further exploration of the potential mechanisms accounting for the growth inhibition effect of cyclometalated Ru(II)-isoquinoline compounds.

Table 1. Cytotoxicity assay *in vitro* (IC<sub>50</sub><sup>\*</sup>) and Log P<sub>o/w</sub> values.

Complexes	IC <sub>50</sub> (μM)					SI <sup>c</sup>	Log P <sub>o/w</sub>
	NCI-H460	A549	MCF-7	HeLa	HBE		
<i>cis</i> -[Ru(bpy) <sub>2</sub> Cl <sub>2</sub> ]	194.2±6.51 <sup>b</sup>	>200	189.2±4.31 <sup>b</sup>	>200	>200	-	-
<i>cis</i> -[Ru(phen) <sub>2</sub> Cl <sub>2</sub> ]	>200	>200	>200	197.5±6.12 <sup>b</sup>	>200	-	-
<b>1-Ph-IQ</b>	172.0±3.9 <sup>b</sup>	>200	194.7±6.1 <sup>ab</sup>	>200	>200	-	-
<b>RuIQ-1</b>	2.1±0.2	3.2±0.1	7.2±0.4	4.3±0.3	22.0±0.8 <sup>a</sup>	10.5	1.02±0.10

<b>RuIQ-2</b>	1.8±0.3	2.5±0.5	7.0±0.3 <sup>a</sup>	4.7±0.4	20.0±0.3 <sup>a</sup>	11.1	1.12±0.09
<b>Ru3</b>	69.1±3.4 <sup>b</sup>	74.5±3.7 <sup>b</sup>	72.0±3.4 <sup>b</sup>	80.2±4.1 <sup>b</sup>	96.1±3.4 <sup>a,b</sup>	1.4	-1.65±0.12
<b>Ru4</b>	77.6±4.1 <sup>b</sup>	79.3±3.8 <sup>b</sup>	88.7±4.7 <sup>b</sup>	82.2±3.5 <sup>b</sup>	97.6±4.2 <sup>a,b</sup>	1.3	-1.07±0.08
Cisplatin	25.9±1.5 <sup>b</sup>	27.3±1.8 <sup>b</sup>	21.8±2.2 <sup>b</sup>	15.0±2.0 <sup>a,b</sup>	16.4±1.9 <sup>a,b</sup>	0.6	ND

\* is the illustrated cells were treated for 48 h, and the data is expressed as mean  $\pm$  standard deviation (Mean  $\pm$  SD). <sup>a</sup> indicates the same complex, different cell groups and NCI-H460 cell group bilateral *t*-test,  $P < 0.05$ ; <sup>b</sup> indicates bilateral *t*-test between the same cell line, different complex treatment groups and complex **RuIQ-2** treatment group,  $P < 0.05$ . <sup>c</sup> SI (Selectivity Index) =  $IC_{50}(\text{HBE})/IC_{50}(\text{NCI-H460})$ .

#### 2.4. Lipophilicity and cellular uptake of Ru(II) complexes

It is generally acknowledged that the lipophilicity of the metal-based agents plays a vital influence on their cellular uptake, cytotoxicity, and subsequent cancer therapeutic [26, 45-47]. In this study, the lipophilicity, expressed as oil-water partition coefficient ( $\log P_{o/w}$ ), is evaluated by the “shake-flask” method using inductively coupled plasma mass spectrometry (ICP-MS). As shown in Fig. 3A, the cyclometalated complexes (**RuIQ-1** and **RuIQ-2**) are more lipophilic than the non-cyclometalated complexes (**Ru3** and **Ru4**), with the order of the  $\log P_{o/w}$  values being recorded: **RuIQ-2** (1.12) > **RuIQ-1** (1.02) > **Ru4** (-1.07) > **Ru3** (-1.65). Complex **RuIQ-2** displayed the highest  $\log P_{o/w}$  value, suggesting that this complex is the most hydrophobic, which may contribute to its highest cytotoxicity. By contrast, complexes **Ru3** and **Ru4** exhibited negative  $\log P_{o/w}$  values, indicating that they are hydrophilic, that is why they gave moderately cytotoxicities. It is very interesting to note that the only difference among complexes **RuIQ-1**, **RuIQ-2**, **Ru3** and **Ru4** is the molecular structure, but they display obvious differences in their  $\log P_{o/w}$  values, and then results in different cytotoxicities.

To investigate the relationship between the cellular uptake rate and the cytotoxicity of **RuIQ-1** and **RuIQ-2**, ICP-MS was performed to quantitative determine of the ruthenium level inside of the NCI-H460 cells, with the results being represented as ng of ruthenium per  $10^6$  cells. Our results showed that a noticeable time- and concentration-dependent increase in the uptake of **RuIQ-1** and **RuIQ-2** by NCI-H460 cells (Fig. 3B). As expected, complex **RuIQ-2** exhibited higher cellular

uptake than that of **RuIQ-1** in all the test time points and drug concentrations, which due to its highest hydrophobicity. The studies of Barton and Chao et al. have illustrated that the most liposoluble Ru(II) complexes presented the greatest uptake [48-50].

When the cellular distribution of complexes **RuIQ-1** and **RuIQ-2** was measured in NCI-H460 cells by ICP-MS, it was evident that, after 6 h incubation using 2  $\mu$ M of the chemicals, **RuIQ-1** and **RuIQ-2** mainly accumulated in the nucleus and mitochondria, with only a small fraction of them detectable in the cytoplasm. Since the cell nucleus contains DNA etc. most of the cellular genetic material, the accumulation of **RuIQ-1** and **RuIQ-2** in the nucleus may cause suppression of cellular DNA transcription and replication, and exhibit their biological activities. These results also indicated that **RuIQ-1** and **RuIQ-2** may mainly target nucleus and mitochondria, similar with the previously reported cyclometalated Ru(II) complexes such as [Ru(bpy)(phpy)(dppz)](ClO<sub>4</sub>) [26] and [Ru(L)<sub>2</sub>(1-Ph- $\beta$ C)](PF<sub>6</sub>) (L=dmb, bpy) [42].

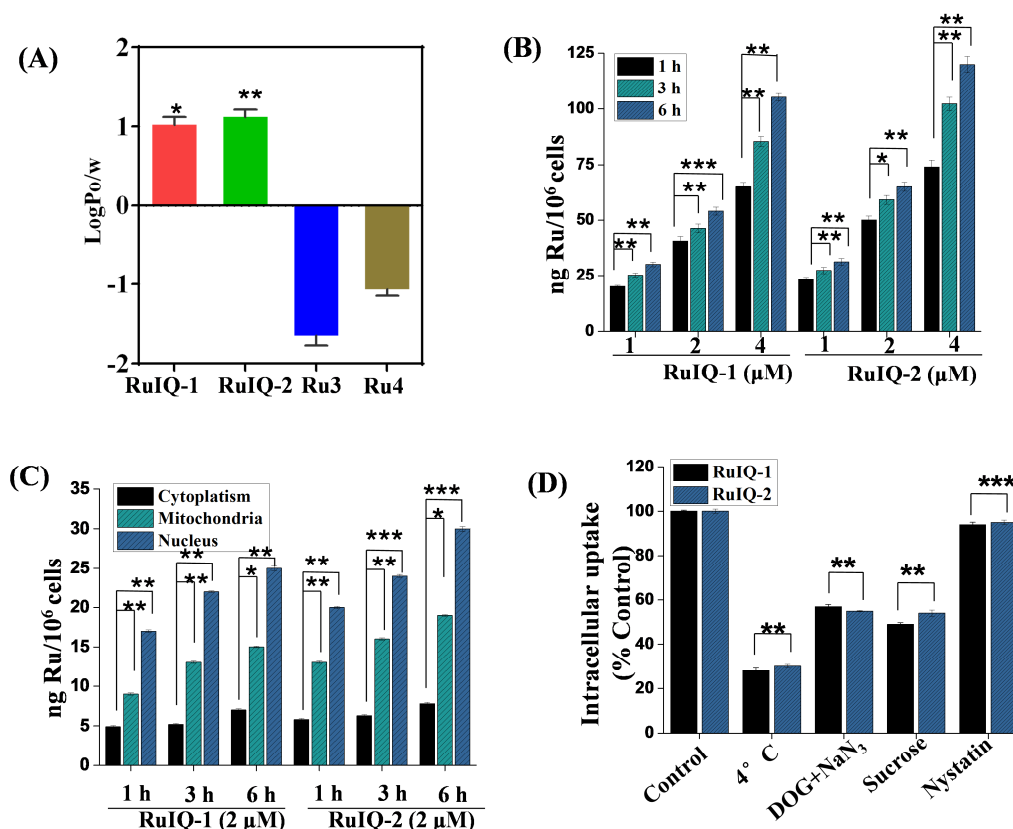


**Fig. 3.** Lipophilicity and cellular uptake of Ru(II) complexes. (A) LogP<sub>o/w</sub> values of Ru(II) complexes. (B) Cellular ruthenium concentrations determined in NCI-H460 cells after 1, 3, and 6 h incubated with **RuIQ-1** and **RuIQ-2** at 1, 2, 4 μM, respectively. (C) Subcellular distribution of Ru(II) complexes in NCI-H460 cells after incubated with **RuIQ-1** (2 μM) or **RuIQ-2** (2 μM) for different period. (D) Intracellular uptake of Ru(II) complexes in NCI-H460 cells under different endocytosis-inhibited conditions. Data were collected from three individual experiments (\*p < 0.05, \*\*p < 0.01, and \*\*\*p < 0.001).

### 2.5. The mechanism of cellular uptake

The ways of drug entering into the cells have an essential impact on their biological activity. Generally, the drug molecules enter cancer cells via active and passive pathways. Active transport is energy dependent, on the contrary, passive transport is a non-energy-dependent way [51]. To gain more insight into the detailed routes of complexes **RuIQ-1** and **RuIQ-2** into cells, we treated NCI-H460 cells with Ru(II) complexes at either low temperature (4 °C) or NaN<sub>3</sub> in combination with DOG, a commonly used strategy to block adenosine 5'-triphosphate (ATP) dependent active mechanisms. The results showed that both low temperature and DOG+NaN<sub>3</sub> could strongly block the cellular uptake of **RuIQ-1** and **RuIQ-2** (Fig. 3D), denoting that

both **RuIQ-1** and **RuIQ-2** are taken up by NCI-H460 cells via active transport pathway. Endocytosis is the most common active transport, and engaged in the cellular uptake of a wide variety of exogenous molecules. In order to further investigate the internalization pathway of **RuIQ-1** and **RuIQ-2**, we used two endocytosis inhibitors, i.e. nystatin (clathrin-mediated endocytosis) and sucrose (lipid raft-mediated endocytosis) [51]. In our study, it was found that the cellular uptake levels of both **RuIQ-1** and **RuIQ-2** were significantly reduced in the sucrose group, with only a moderate decrease in the nystatin group. These results manifest that the cross-membrane transportation of **RuIQ-1** and **RuIQ-2** mainly via the clathrin-mediated endocytosis pathway.

#### 2.6. Cyclometalated Ru(II) complexes induce apoptosis in NCI-H460 cells

Apoptosis has been observed to engage in the anti-cancer activity of many of the previously reported drugs [52-54]. Next, the Hoechst 33342 staining technique, accompanied by fluorescence microscopy assay were performed to determine whether such a mechanism involved in the potential anti-cancer effect of the complexes **RuIQ-1** and **RuIQ-2**. As shown in Fig. 4A and 4B, after **RuIQ-2** treatment, the NCI-H460 cells showed noticeable apoptotic morphology, including nuclear shrinkage and chromatin condensation, in a time- and concentration-dependent manner. Similar apoptotic features were also observed after **RuIQ-1** treatment (Fig. S14A). These results strongly suggested that the involvement of apoptosis in the Ru(II) complexes-mediated cell death.

To provide further information about Ru(II) complexes-mediated cell death, Annexin V/PI staining was performed, and the results were analyzed by Flow Cytometry. We can clearly observe that the Ru(II) complexes induced apoptosis of the NCI-H460 cells in a concentration-dependent manner (Fig. 4C and Fig. S14B). Differing from the control group, where the percentage of the early apoptotic cells recorded 2.24% and 1.73%, after the cells were incubated with **RuIQ-1** and **RuIQ-2** at 4  $\mu$ M for 24 h, the percentage of early apoptotic cells increased to 42.96% for

**RuIQ-1** and 57.31% for **RuIQ-2**. Comparing the apoptotic effect, it was clear that the complex **RuIQ-2** displayed more effective apoptotic activity than **RuIQ-1**, with the percentage of total apoptotic cells recorded 51.23% for **RuIQ-1** and 68.05% for **RuIQ-2**. This observation is consistent with their cytotoxic activity. Since complex **RuIQ-2** presents more effective growth inhibition and apoptosis induction effects in the NCI-H460 cells than that of **RuIQ-1**, the apoptosis-induced mechanism of it was further investigated.

Apoptotic pathways can be divided into the intrinsic and extrinsic ways according to which caspases are involved [55]. As an essential regulatory protein in the downstream pathway of apoptosis, caspase plays a vital role in the initiation and performance of apoptosis. Caspase, especially caspase-3 activation, subsequently can lead to the cleavage of poly ADP-ribose polymerase (PARP), serving as a biochemical marker of cells apoptosis [56]. To investigate the molecular events initiated by **RuIQ-2**, after treatment for 24 h, the activities of caspase-3, -8 and -9 were analyzed by western blot assay. According to Fig. 4D, co-incubation with 1, 2, and 4  $\mu\text{M}$  of **RuIQ-2** for 24 h caused a significant in the protein expression levels of the cleaved-PARP, cleaved caspase-3, -8 and -9. Meanwhile, with the shearing of caspase-8, caspase-9, caspase-3 and PARP, the total expression levels of caspase-3 and PARP experienced a significant declined. All these findings demonstrated that **RuIQ-2**-induced apoptosis in NCI-H460 cells through caspase-dependent extrinsic and intrinsic pathways.

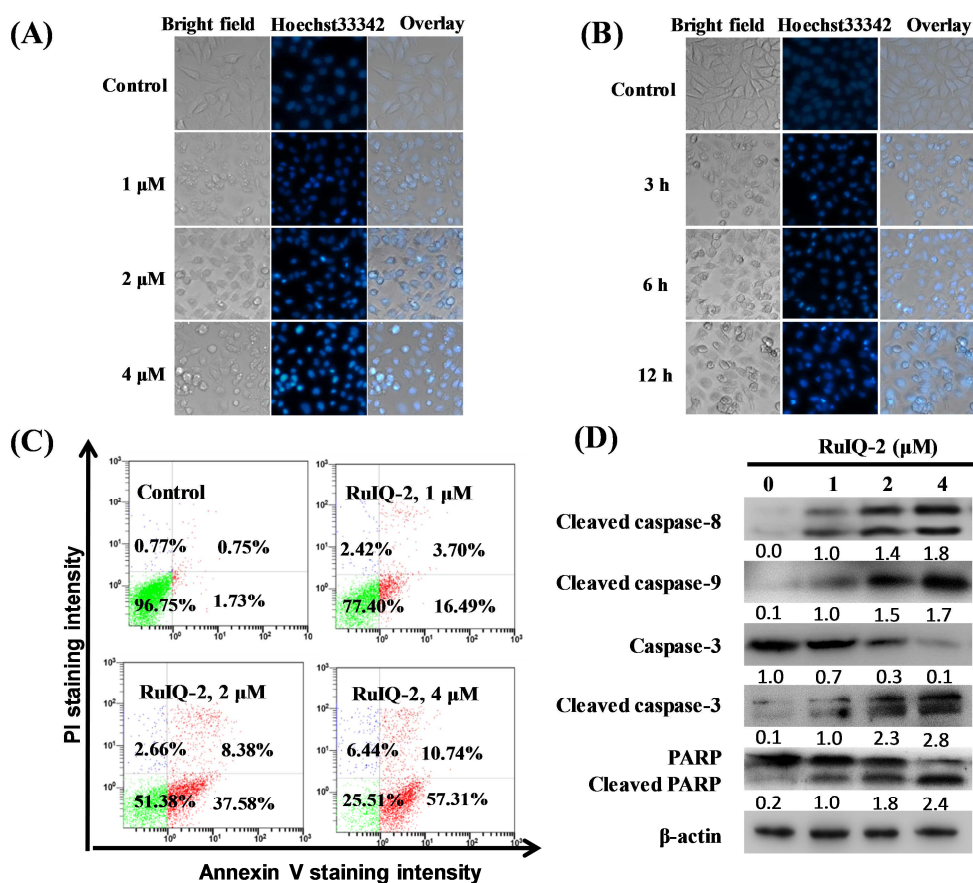


**Fig. 4.** RuIQ-2 induced apoptosis in NCI-H460 cells. (A) NCI-H460 cells were stained with Hoechst 33342 after co-incubation with 1, 2, and 4  $\mu\text{M}$  of RuIQ-2 for 12 h. (B) NCI-H460 cells were stained with Hoechst 33342 after co-incubation with RuIQ-2 at 2  $\mu\text{M}$  for different time. (C) NCI-H460 cells apoptosis was detected by Annexin V/PI assay after treatment with 1, 2, and 4  $\mu\text{M}$  of RuIQ-2 for 24 h. (D) The expression of Cleaved caspase-9, -8, -3, caspase-3, PARP, Cleaved PARP were evaluated by western blot analysis in a concentration-dependent manner with RuIQ-2 treatment for 24 h.

### 2.7. Cyclometalated Ru(II) complexes induce mitochondrial dysfunction

Since mitochondrion can release pro-apoptotic factors such as cytochrome *c* and other apoptosis-inducing factors, hence, it plays a vital role in the apoptotic process [52-54, 57]. To investigate the effects of Ru(II) complexes on mitochondrial membrane potential (MMP), decline of which is a marker of mitochondrial dysfunction, the changes in MMP were detected by the fluorescent probe 5,5',6,6'-tetrachloro-1,1',3,3'-tetraethylbenzimidazolylcarbo cyanine iodide (JC-1). When MMP is low, JC-1 monomer emits green fluorescence signal, while when MMP is high, JC-1 aggregate displays red fluorescence signal. In our study, after treatment

with 1, 2, and 4  $\mu\text{M}$  of **RuIQ-1** or **RuIQ-2** for 12 h, the red fluorescence saw prominent decrease while significant increase in the green fluorescence occurred (Fig. 5A and Fig. S15A). Similar results were recorded when treatment with 2  $\mu\text{M}$  of **RuIQ-1** or **RuIQ-2** for a series of different time points (Fig. 5B and Fig. S15B). All these findings indicate the decline of MMP. In addition, for **RuIQ-2**, the changes of MMP were detected quantitatively by using flow cytometry (Fig. 5C, D). As presented in Fig. 5C, after treatment with **RuIQ-2** for 12 h, the green fluorescence of the JC-1 monomers increased from 16.0% (1  $\mu\text{M}$ ) to 56.7% (4  $\mu\text{M}$ ). The decline of MMP is also a marker of apoptosis. To further confirm the mitochondrial pathways in **RuIQ-2**-induced apoptosis, we detected the expression of Bcl-2, Bax, Bcl-xl, and Bad in mitochondrial membrane and cytochrome *c* protein in cytoplasm using western blot analysis. As shown in Fig. 5E, with the increase of **RuIQ-2** concentration, the expression of Bcl-2 and Bcl-xl (anti-apoptotic proteins) showed notable attenuation. At the same time, the expression of Bax and Bad (pro-apoptotic proteins), as well as the content of cytochrome *c* protein in the cytoplasm experienced a significant increase. These results collectively indicated that **RuIQ-2** induced apoptosis in NCI-H460 cells through the mitochondrial apoptotic pathway.

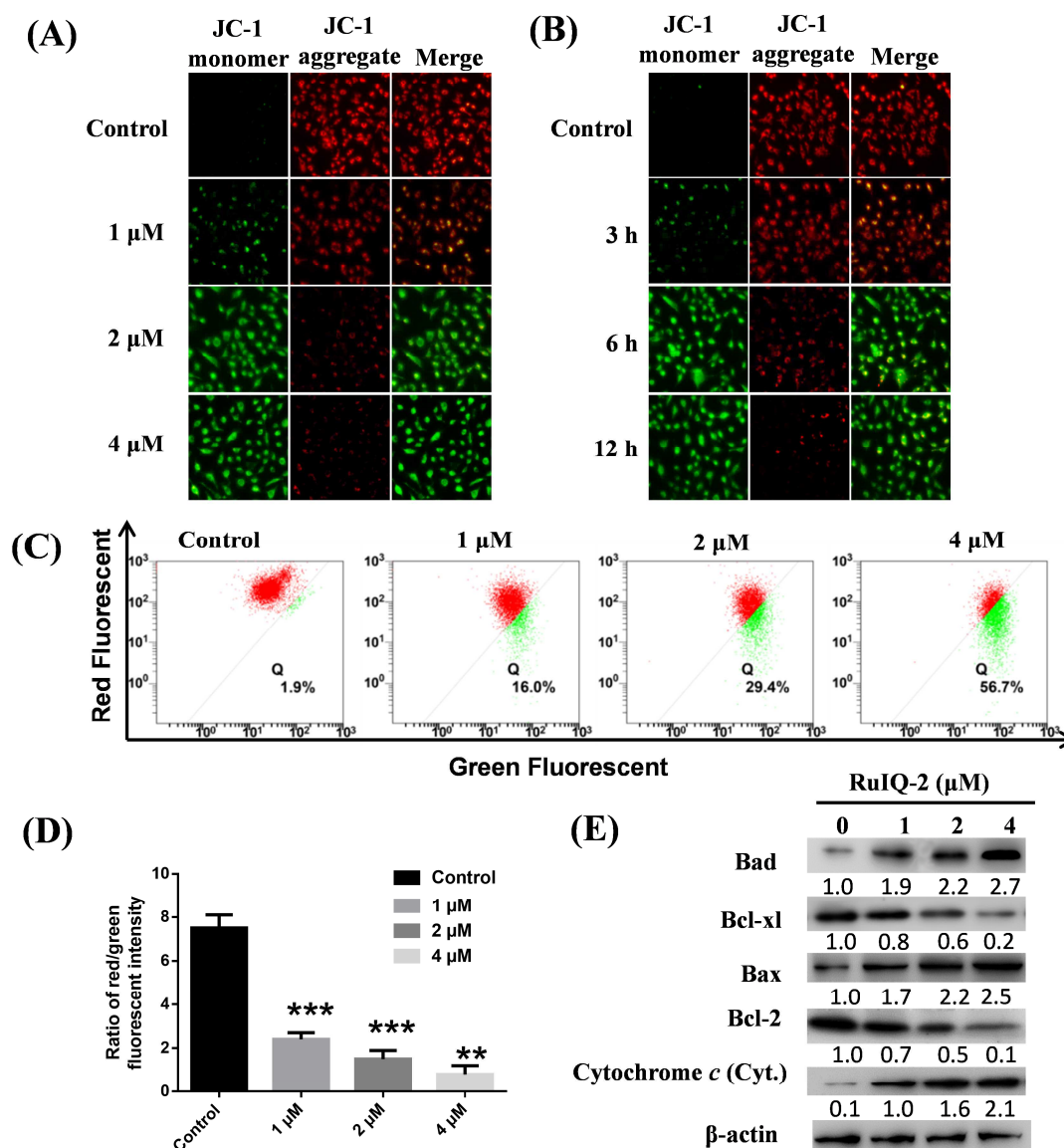


**Fig. 5.** RuIQ-2 induced mitochondrial dysfunction in NCI-H460 cells. (A) Fluorescence microscopy analysis of cellular MMP level by JC-1 staining after treatment with RuIQ-2 at 1, 2 and 4  $\mu$ M for 12 h. (B) Fluorescence microscopy analysis of cellular MMP level by JC-1 staining after 2  $\mu$ M of RuIQ-2 treatment for different time. (C) Flow cytometry analysis of cellular MMP level after treatment with RuIQ-2 at 1, 2 and 4  $\mu$ M for 12 h. (D) Flow cytometry analysis the ratio of red/green fluorescent intensity after treatment with RuIQ-2 at 1, 2 and 4  $\mu$ M for 12 h. Data were collected from three individual experiments (\*  $p < 0.05$ , \*\*  $p < 0.01$ , and \*\*\*  $p < 0.001$ ). (E) Western blot analysis of the expression levels of Bcl-2, Bax, Bcl-xl, Bad in mitochondrial membrane and cytochrome *c* protein in cytoplasm after RuIQ-2 (2  $\mu$ M) treatment for 24 h.

## 2.8. Cyclometalated Ru(II) complexes stimulate the generation of intracellular ROS

It has been demonstrated that ROS could induce a chain of mitochondria-associated events, such as the decline of MMP and apoptosis [52-54,

57]. Hence, ROS is considered to be a mediator of apoptosis [58, 59], and exploring the cellular ROS levels is of great importance to elucidate the underlying mechanism of Ru(II) complexes-induced apoptosis. To investigate whether Ru(II) complexes stimulate ROS generation and accumulation, 2,7-dichloride-hydrofluorescein diacetate (DCFH-DA) fluorescent probe-based imaging assay was performed. We observed that the fluorescence intensity in NCI-H460 cells both increased in a time- and concentration-dependent manner after **RuIQ-1** or **RuIQ-2** treatment (Fig. S16 and S17), suggesting the generation and accumulation of ROS. Moreover, the cellular ROS level was further measured by flow cytometry after **RuIQ-2** treatment. As shown in Fig. 6A and Fig. S18, after 12 h of co-incubation with 1, 2, and 4  $\mu\text{M}$  of **RuIQ-2**, a noticeable enhanced in the mean fluorescent intensity (M) was observed, with the DCF fluorescence increased from 1.31 to 6.51, which is approximately 5-fold higher than that of the control group. So we came to the conclusion that the cyclometalated Ru(II) complexes could induce the generation of ROS in NCI-H460 cells.

As reported, the ROS can be generated either endogenously during the process of mitochondrial oxidative phosphorylation, or produced from the interaction between exogenous sources such as xenobiotic compounds [60]. So, mitochondria are both source and target of ROS [61]. The cyclometalated complexes studied in this work can induce the decline of mitochondrial membrane potential (MMP) and results in mitochondrial dysfunction, which causes the damage of respiratory chain, and generates radical and non-radical species such as superoxide anion ( $\text{O}^{2-}$ ) and hydrogen peroxide ( $\text{H}_2\text{O}_2$ ). Based on the above information, these cyclometalated Ru(II) complexes may stimulate the mitochondria based ROS generation. This speculation correlates with our previous publication [58], the Ru(II) complex-triggered ROS generation could be effectively blocked by using cyclosporine A (CsA), a confirmed mitochondrial permeability transition pore (MPTP) opening inhibitor.

To further explore the effect of ROS activation induced by complex **RuIQ-2** on

mitochondria and cell apoptosis, two ROS inhibitors, i.e. glutathione (GSH) and N-acetyl-l-cysteine (NAC), were used in our study. After the addition of either NAC or GSH, the fluorescence intensity of DCF displayed significant reduction (Fig.S19), indicating the inhibition of ROS generation in NCI-H460 cells. Next, NCI-H460 cells were treated with 2  $\mu\text{M}$  of **RuIQ-2** combined with/without GSH (5 mM) or NAC (10 mM) for 12 h. After stained with Annexin V-FITC/PI, the percentage of apoptotic cells was measured using flow cytometry. From Fig. 6B and Fig. 6C, it was evident that both NAC and GSH could block **RuIQ-2**-induced apoptosis in NCI-H460, denoting that ROS generation played an essential role in **RuIQ-2**-induced apoptosis in the tested NCI-H460 cells. This mechanism was further demonstrated by subsequent western blot assay. The results in Fig. 6D manifested that pretreatment of NAC or GSH inhibited cytochrome *c* release in the cytoplasm and efficiently reversed the **RuIQ-2**-induced PARP and caspase-3 phosphorylation. The implication of all these is that **RuIQ-2**-induced apoptosis in NCI-H460 cells is triggered by ROS-mediated mitochondrial dysfunction.

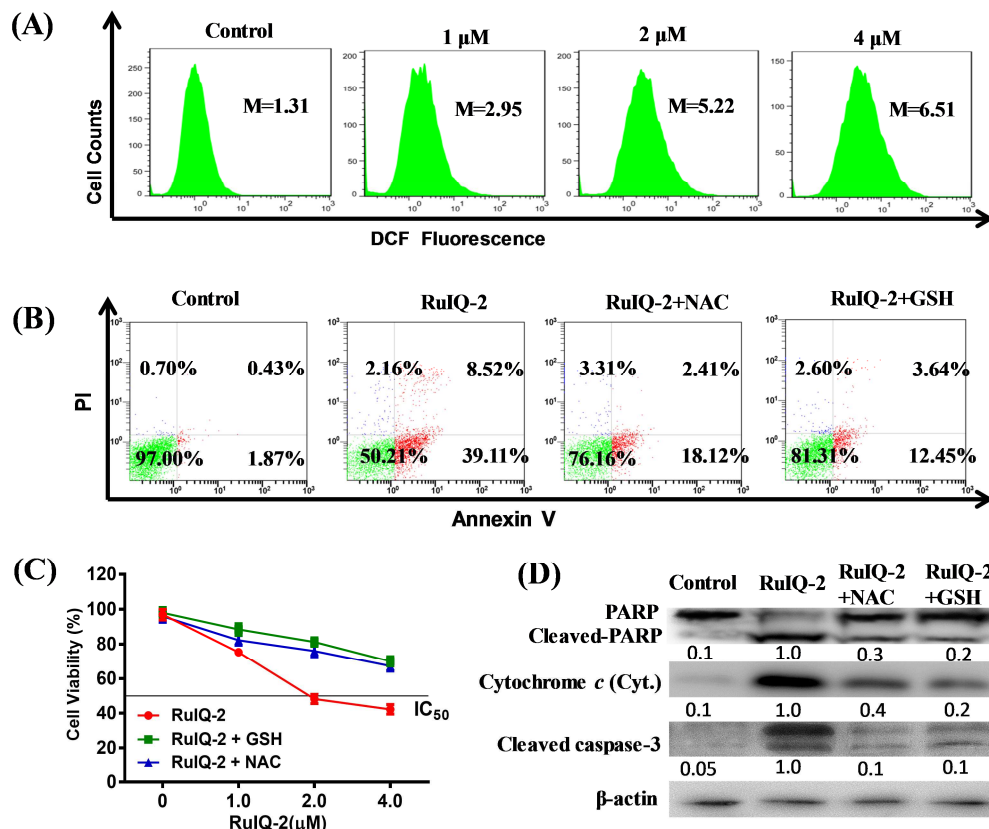


**Fig. 6. RuIQ-2** stimulated generation of intracellular ROS. (A) Flow cytometry analysis of cellular ROS level by DCFH-DA staining in a concentration-dependent manner upon **RuIQ-2** treatment for 12 h. (B) The percentage of apoptotic cells were detected by Annexin V-FITC/PI double staining assay using flow cytometry after 2  $\mu\text{M}$  **RuIQ-2** treatment with or without antioxidants NAC (10 mM) or GSH (5 mM). (C) Cell viability was assessed by MTT assay after 12 h of **RuIQ-2** treatment with or without NAC (10 mM) or GSH (5 mM). (D) Western Blot analysis of the protein expression levels of PARP, cytochrome *c* and cleaved caspase-3 after **RuIQ-2** (2  $\mu\text{M}$ ) treatment for 24 h with or without NAC (10 mM) or GSH (5 mM).

### 2.9. Cyclometalated Ru(II) complexes trigger DNA damage and S, G2/M double-cycle arrest

DNA damage, such as the change of cellular DNA structure, can lead to inhibition of DNA replication. When DNA damage cannot be repaired, it may cause cell cancer. So, DNA damage is considered as a mark of apoptosis [62-65]. We have reported that many Ru(II) complexes could promote the generation of cellular ROS levels, which in turn attack DNA and results in apoptosis [42, 51, 66, 67]. To determine whether or not these complexes can induce DNA damage, the single-cell gel electrophoresis assay (comet assay) was conducted in our study. As shown in Fig. S20A and Fig. 7A, in the control group, NCI-H460 cells failed to show a comet-like appearance. However, after **RuIQ-1** (1  $\mu\text{M}$ ) or **RuIQ-2** (1  $\mu\text{M}$ ) treatment for 12 h, NCI-H460 cells exhibited well-formed comet tails, indicating the existence of severe DNA damage. When the treatment concentration was increased to 4  $\mu\text{M}$ , significantly prolonged comet tails appeared, denoting that more DNA damage occurred with the increase of complexes concentration. Furthermore, it was also found that NCI-H460 cells presented well-formed comet tails in a time-dependent manner after 2  $\mu\text{M}$  of **RuIQ-2** treatment (Fig. 7B). To provide solid evidence about the **RuIQ-2**-induced DNA damage, western blot analysis was scheduled (Fig. 7C and 7D). Coincident with our previous reports, **RuIQ-2** treatment resulted in significantly up-regulated DNA damage markers, including the phosphorylation levels of ATM (Ser1984), Histone H2A.X (Ser139), ATR (Ser 428) and p53 (Ser15) [42, 51]. Meanwhile, the phosphorylation levels of Chk1 and Chk2 were also up-regulated. Moreover, several cell cycle arrest-related key downstream proteins (e.g. p21, p27) were simultaneously activated

(Fig.7D).

The comet tail observed does not mean that the ruthenium complexes directly damage DNA. It has been reported that excess intracellular ROS could attack DNA, resulting in DNA damage [68, 69]. So, the observed DNA damage may result from the increased intracellular ROS levels. This has been confirmed by our previous study (the cyclometalated Ru(II)  $\beta$ -carboline complexes could induce DNA damage through ROS overproduction [42]. Many Ru(II) complexes can bind to DNA in a noncovalent interaction such as electrostatic binding, groove binding, or intercalation [70-73]. We didn't do DNA-binding experiments in this work. However, according to our previous studies [42, 66, 74, 75], we speculate that the binding affinity of the title complexes towards DNA is not very strong because they don't have a large planar aromatic ligand (intercalative), such as dppz, dpq and pip [66, 74, 75], so the interaction between them and DNA is not supposed to be the primary reason of apoptosis.

From the biology aspects, DNA is the key information carrier, so it is highly stable over the evolution, except for the DNA enzyme mediated degradation. Differing from necrosis mediated cell death, which is caused by external factors such as trauma or infection, the apoptosis, featured by fragmentation of nuclei, is a secondary response to DNA damage, with the biological goal of protecting a multicellular organism against a damaged cell. As a result, the apoptosis mediated cell death has been commonly measured using the comet assay to detect DNA damage of cells after treatment with complexes. Comets with almost all DNA in the tail are often referred to as 'hedgehog' comets and are widely assumed to represent apoptotic cells. In summary, the title complexes could induce mitochondrial dysfunction and the generation of intracellular ROS, which may indirectly lead to DNA damage. Also, the comet assay (DNA fragments appearance) could serve as a mark for apoptosis assessment.

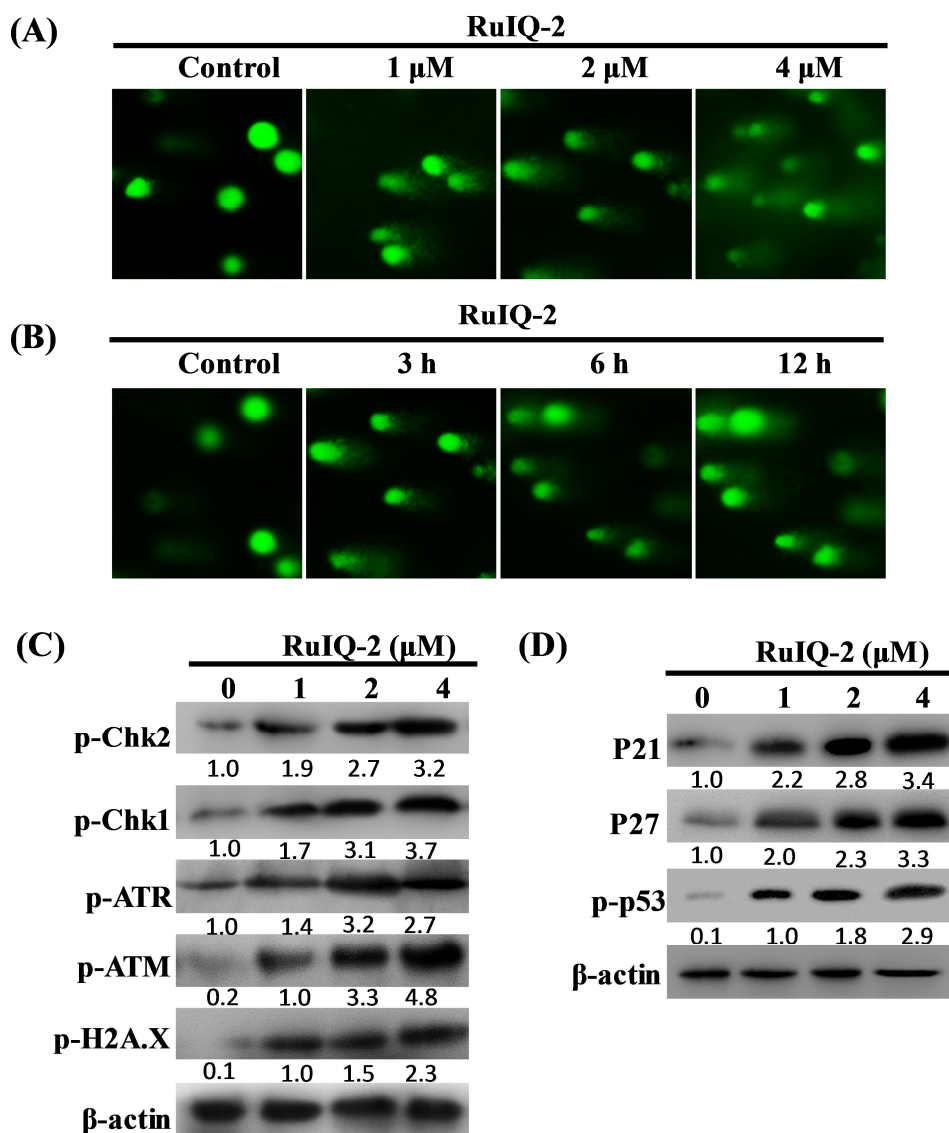


**Fig. 7. RuIQ-2 induced DNA damage in NCI-H460 cells.** (A) DNA fragmentation was examined by comet assay. NCI-H460 cells were treated with **RuIQ-2** at 1, 2 and 4  $\mu$ M for 12 h. (B) DNA fragmentation of NCI-H460 cells was examined, after treatment with **RuIQ-2** (2  $\mu$ M) for different time period (3, 6, 12 h). (C) The level of DNA damage proteins (p-Histone H2A.X, p-ATM, p-ATR, p-Chk1, p-Chk2) were assessed by western blot analysis, after treatment with **RuIQ-2** at 1, 2 and 4  $\mu$ M for 24 h. (D) Western blot analysis of the expression level of p-p53, p27, p21, after treatment with various concentration of complex **RuIQ-2** for 24 h.

DNA damage can directly affect DNA transcription, replication and cell cycle arrest. To investigate whether the DNA damage caused by studied complexes on NCI-H460 cells could affect cell cycle distribution of NCI-H460 cells, the cell cycle ratio was detected by flow cytometry. The results in Fig. 8A and Fig. 8B displayed that, after treating with **RuIQ-2** at 4  $\mu$ M for 24 h, compared with the control group,

the cell proportion of S phase nearly doubled, increased from 18.22% to 33.83%. A similar trend was observed for the G<sub>2</sub>/M phase, which increased from 11.44% to 26.29%. These data suggested that **RuIQ-2** could induce cell cycle arrest at S and G<sub>2</sub>/M phases in NCI-H460 cells. Similar S, G<sub>2</sub>/M double-cycle arrest results were also observed in NCI-H460 cells after **RuIQ-1** treatment (Fig. S20B).

As we all know, cell-cycle progression is regulated by forming a series of specialized cyclin-dependent kinase (CDK)-cyclin complexes. To explore the mechanism of **RuIQ-2**-induced cell cycle arrest, western blot analysis was employed to examine the effect of **RuIQ-2** treatment on the expression of regulatory proteins, such as CDK2/Cyclin A, CDK1/Cyclin B. Our results showed that, after **RuIQ-2** treatment, the expression of CDK1 and Cyclin B (key factors of G<sub>2</sub>/M phase arrest) [76, 77] significantly down-regulated (Fig. 8C). Although no apparent change of CDK2 was observed, the expression of Cyclin A saw a prominent decrease. Since the formation of CDK2-Cyclin A complex has been confirmed to be closely related to phase S arrest [78], the reduction of Cyclin A expression definitely contributes to the effect of **RuIQ-2**. Moreover, as shown in Fig.7D, both p21 and p27, two of the well-known CDK inhibitors contributing to the G<sub>1</sub>-S transition blockage, also displayed up-regulation [78, 79]. All of these findings demonstrated that both **RuIQ-1** and **RuIQ-2** could trigger DNA damage and S, G<sub>2</sub>/M double-cycle arrest via suppressing the expression of regulatory proteins CDK1/Cyclin B and Cyclin A.

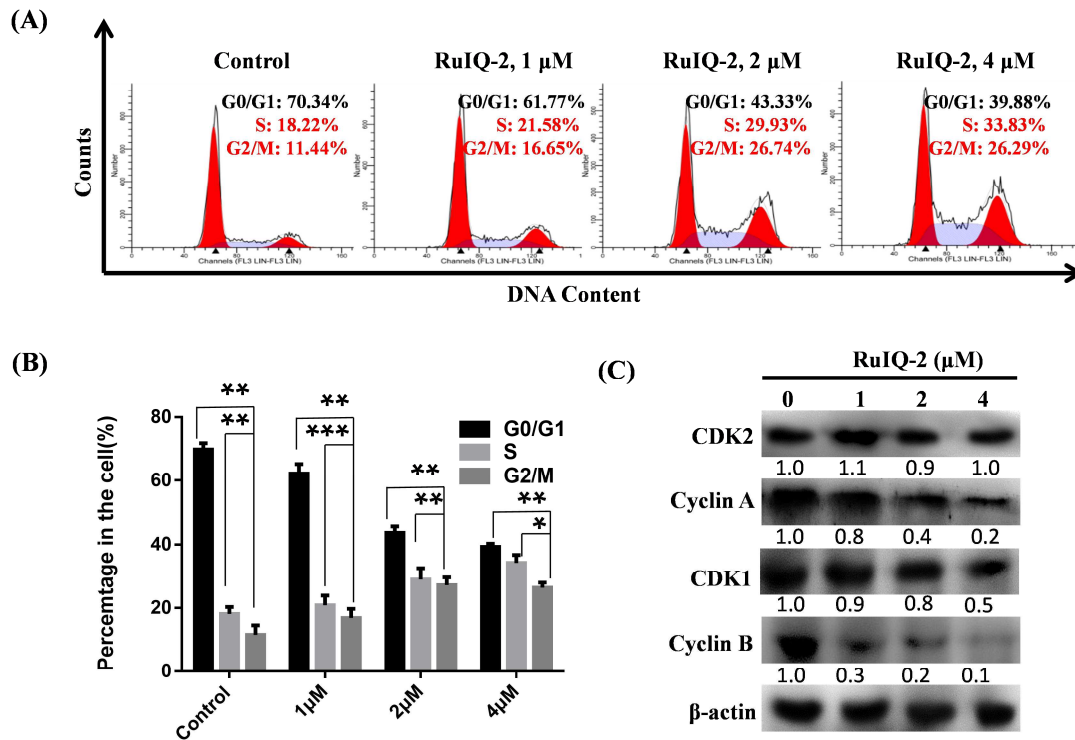


**Fig. 8. RuIQ-2 induced cycle arrest in NCI-H460 cells.** (A) Cell cycle distribution was performed by PI staining after co-incubated with **RuIQ-2** for 24 h. (B) Histograms show cell cycle distribution of the NCI-H460 cells. Data were collected from three individual experiments (\*  $p < 0.05$ , \*\*  $p < 0.01$ , and \*\*\*  $p < 0.001$ ). (C) Western blot analysis of expression of CDK1, CDK2, Cyclin A, and Cyclin B. NCI-H460 cells were treated with **RuIQ-2** at 1, 2 and 4  $\mu\text{M}$  for 24 h.

### 2.10. Complex RuIQ-2 shows low toxicity to developing zebrafish embryos

Compared with athymic nude mice models, zebrafish has potential advantages, such as high reproductive rate and short growth period, etc. Recently, zebrafish has rapidly developed to be a promising model for evaluating the toxicity of drugs [80-82]. In this work, the *in vivo* toxicity of complex **RuIQ-2** was assessed on developing zebrafish embryos.

As displayed in Fig. 9A, after exposure to **RuIQ-2** at the expected treatment concentrations (less than 16  $\mu\text{M}$ ), only minor toxicity was observed, with most of the zebrafish embryos developing into juvenile zebrafish (more than 80% cumulative hatch rate after 72 h) (Fig. 9B). And under such a concentration, the lethality rate was lower than 40% even after prolonged 96 h incubation (Fig. 9C). When the concentration of **RuIQ-2** increased to 16  $\mu\text{M}$  for 96 h, we observed that some zebrafish embryos developed abnormally with a marked spinal curvature (Fig. 9A).

Moreover, when **RuIQ-2** concentration was increased to 32  $\mu\text{M}$ , a cumulative hatch rate of less than 50% was recorded after 48 h incubation, and all the zebrafish embryos died at the time point of 96 h. Therefore, it looks like that under the effective concentration range (less than 16  $\mu\text{M}$ ), **RuIQ-2** was generally safe for zebrafish embryos. Since hypotoxicity to normal cells or organs is vital for developing novel anticancer agents, complex **RuIQ-2** is expected to be developed as a low-toxicity agent against lung cancer cells.

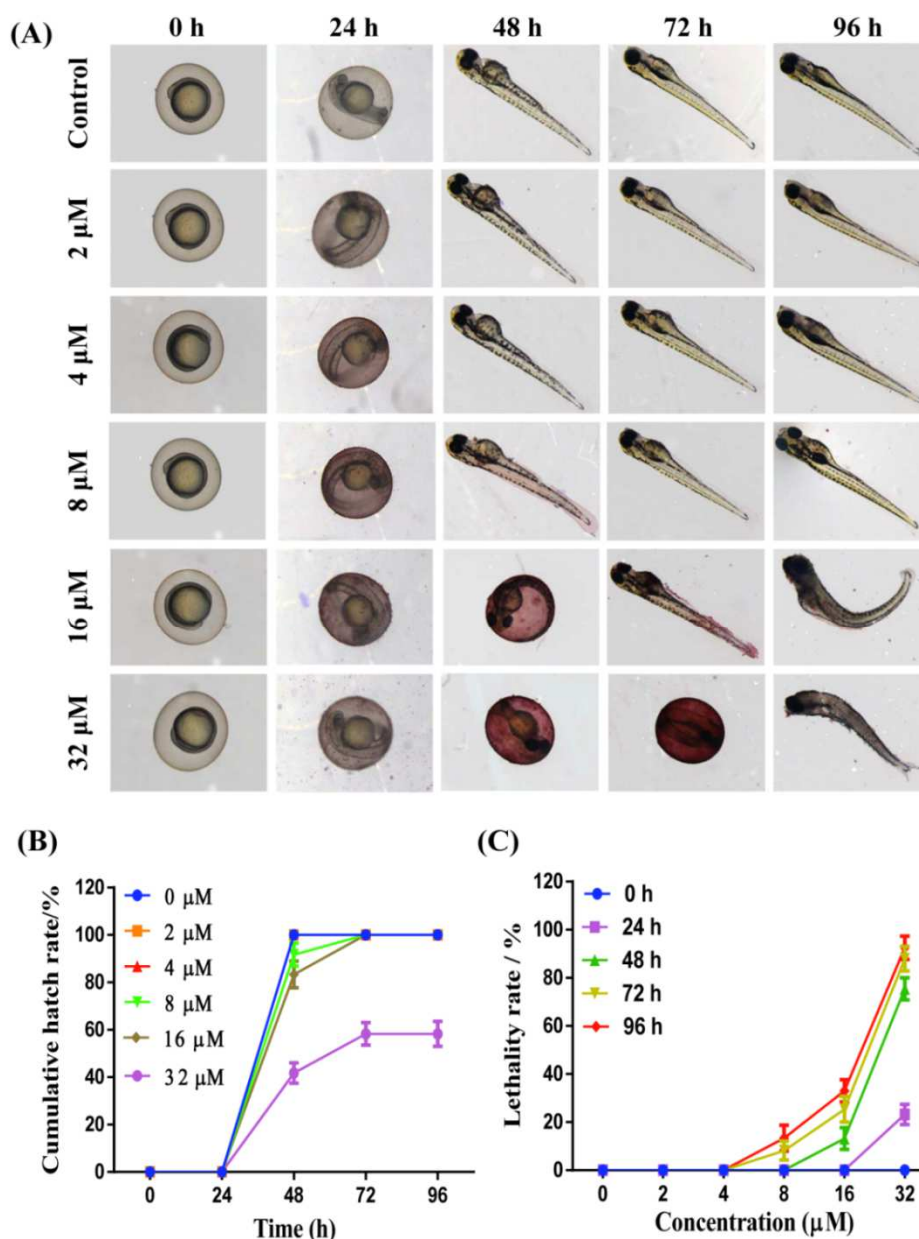


**Fig. 9.** Toxicity assessment of **RuIQ-2** in developing zebrafish embryos. (A) Toxicity of **RuIQ-2** to zebrafish embryos at various concentrations within 96 h on a 4 $\times$  objective lens in the microscope. (B) Cumulative hatch rate of zebrafish embryos in the presence/absence of **RuIQ-2** at

various concentrations every 24 h. (C) Lethality rate of zebrafish embryos in the presence/absence of **RuIQ-2** at different concentrations every 24 h.

### 3. Conclusions

Two new cyclometalated Ru(II) complexes, i.e.  $[\text{Ru}(\text{bpy})_2(1\text{-Ph-IQ})]^+$  (**RuIQ-1**) and  $[\text{Ru}(\text{phen})_2(1\text{-Ph-IQ})]^+$  (**RuIQ-2**), have been designed and synthesized. The significant difference in the cytotoxicity between the cyclometalated Ru(II) complexes **RuIQ-1**, **RuIQ-2** and the non-cyclometalated complexes **Ru3**, **Ru4** is due to the obvious difference of lipophilicity caused by the small difference of their molecular structure, i.e., substituting Ru-N with Ru-C bond. Our results suggested that the coordination of the cyclometalated ligand 1-Ph-IQ to polypyridyl-Ru(II) centers can effectively enhance cytotoxicity, and therefore providing a guideline for future anti-cancer complexes exploration.

Our results indicated that **RuIQ-2** could effectively induce S, G2/M double-cycle arrest via suppressing the expression of regulatory proteins CDK1/Cyclin B and Cyclin A. The mechanism studies showed that **RuIQ-2**-induced apoptosis is triggered by ROS-mediated mitochondrial dysfunction. In a word, the Ru (II) complexes can induce apoptosis of NCI-H460 cells by increasing intracellular ROS level, reducing MMP and triggering DNA damage. More importantly, **RuIQ-2** exhibited low toxicity both toward normal HBE cells *in vitro* and zebrafish embryos *in vivo*. Although this work is an *in vitro* assay, further *in vivo* assay using tumour bearing animal models has been scheduled. Based on the current results, the cyclometalated Ru(II) complexes developed in this work has great potential to be developed as novel lung cancer therapeutic agents with fewer side effects.

### 4. Experimental section

#### 4.1. Chemicals and reagents

Ultrapure MilliQ water was used in all experiments. DMSO, MTT, PBS, JC-1, DCFH-DA, PI, Hoechst 33342, NAC, GSH, Annexin V-FITC Apoptosis Detection

Kit, QuantiPro™ BCA Assay Kit, ECL™ Start Western Blotting Detection Reagent and endocytosis inhibitors including NaN<sub>3</sub>, DOG, Sucrose and Nystatin were purchased from Sigma-Aldrich (St. Louis, MO, USA). NCI-H460, A549, HeLa, MCF-7 and HBE cells were purchased from American Type Culture Collection (ATCC, Manassas, VA). Cisplatin was purchased from Acros. Ruthenium standard solution was purchased from Aladdin Chemistry Co. (Shanghai, China). Cell Mitochondria Isolation Kit was purchased from Beyotime (Shanghai, China). Antibodies were purchased from Cell Signaling Technology Company. Comet assay reagent kit was purchased from Trevigen (Gaithersburg, MD, USA).

#### 4.2. Synthesis and characteristics

1-Ph-IQ [39] and *cis*-[Ru(L)<sub>2</sub>Cl<sub>2</sub>]·2H<sub>2</sub>O (L=bpy, phen) [40, 41] were prepared according to the methods in the literature.

Microanalyses were carried out with a Perkin-Elmer 240Q elemental analyzer. Electrospray ionization mass spectrometry (ESI-MS) was recorded on Agilent LC-MS6430B Spectrometer. <sup>1</sup>H NMR spectra were recorded on a Bruker AVANCE AV 400 NMR spectrometer using (CD<sub>3</sub>)<sub>2</sub>SO as solvent at room temperature and TMS as the internal standard. UV-Vis spectra were recorded on a Perkin-Elmer Lambda-850 spectrophotometer (PerkinElmer, USA).

##### 4.2.1. Synthesis of [Ru(bpy)<sub>2</sub>(1-Ph-IQ)](PF<sub>6</sub>) (**RuIQ-1**)

A mixture of *cis*-[Ru(bpy)<sub>2</sub>Cl<sub>2</sub>]·2H<sub>2</sub>O (0.24 g, 0.5 mM), 1-Ph-IQ (0.10 g, 0.5 mM), Ag(CF<sub>3</sub>SO<sub>3</sub>) (0.26 g, 1 mM) and tetramethylammonium hydroxide (0.05 mL, 0.5 mM) in anhydrous ethanol (10 mL) was refluxed under argon at 78 °C for 12 h to produce a clear red solution. After the reaction, the red precipitate was obtained by a dropwise addition of saturated aqueous KPF<sub>6</sub> solution. Finally, the red precipitate was dried under vacuum and purified by column chromatography on neutral alumina with a mixture of CH<sub>3</sub>CN-toluene (3:1, v/v) as eluent. Yield: 76%. Anal. Calc for C<sub>35</sub>H<sub>26</sub>F<sub>6</sub>N<sub>5</sub>PRu: C 55.12%, H 3.44%, N 9.18%; Found: C 55.23%, H 3.41%, N

9.20%. ESI-MS (MeCN):  $m/z = 617.79$  ( $[M-PF_6]^+$ ).  $^1H$  NMR (400 MHz, DMSO- $d_6$ )  $\delta$  8.94 (dd,  $J = 7.3, 2.3$  Hz, 1H), 8.79 (dt,  $J = 8.4, 1.1$  Hz, 1H), 8.78 – 8.60 (m, 3H), 8.36 (d,  $J = 7.9$  Hz, 1H), 8.21 – 8.07 (m, 1H), 8.00 – 7.72 (m, 8H), 7.64 (ddd,  $J = 6.3, 2.2, 1.1$  Hz, 2H), 7.59 (ddd,  $J = 7.5, 5.4, 1.2$  Hz, 1H), 7.47 (d,  $J = 1.0$  Hz, 2H), 7.44 – 7.27 (m, 3H), 6.96 (ddd,  $J = 8.1, 7.1, 1.4$  Hz, 1H), 6.85 (td,  $J = 7.2, 1.2$  Hz, 1H), 6.53 (dd,  $J = 7.5, 1.3$  Hz, 1H). UV-Vis ( $\lambda/nm, \epsilon/M^{-1}$ )(PBS): 297(49200), 505(9550).

#### 4.2.2. Synthesis of $[Ru(phen)_2(1-Ph-IQ)](PF_6)$ (**RuIQ-2**)

Complex **RuIQ-2** was synthesized in a manner identical to that described for **RuIQ-1**, with  $[Ru(phen)_2Cl_2] \cdot 2H_2O$  in place of  $[Ru(bpy)_2Cl_2] \cdot 2H_2O$ . Yield: 71%. Anal. Calc for  $C_{39}H_{26}F_6N_5PRu$ : C 57.78%, H 3.23%, N 8.64%; Found: C 57.70%, H 3.25%, N 8.60%. ESI-MS ( $CH_3CN$ ):  $m/z = 665.81$  ( $[M-PF_6]^+$ ).  $^1H$  NMR (400 MHz, DMSO- $d_6$ )  $\delta$  8.96 (d,  $J = 8.3$  Hz, 1H), 8.69 (dd,  $J = 8.2, 1.4$  Hz, 1H), 8.63 – 8.45 (m, 3H), 8.39 (d,  $J = 8.0$  Hz, 1H), 8.35 – 8.20 (m, 5H), 8.10 (ddd,  $J = 5.4, 3.9, 1.3$  Hz, 2H), 7.93 (dd,  $J = 7.6, 1.9$  Hz, 1H), 7.89 – 7.64 (m, 6H), 7.60 (dd,  $J = 8.1, 5.3$  Hz, 1H), 7.52 (d,  $J = 6.3$  Hz, 1H), 7.40 – 7.34 (m, 1H), 6.95 (ddd,  $J = 8.1, 7.1, 1.4$  Hz, 1H), 6.76 (td,  $J = 7.3, 1.2$  Hz, 1H), 6.43 (dd,  $J = 7.6, 1.3$  Hz, 1H). UV-Vis ( $\lambda/nm, \epsilon/M^{-1}$ )(PBS): 267(54800), 496(11800).

#### 4.2.3. Synthesis of $[Ru(bpy)_2(1-Py-IQ)](PF_6)_2$ (**Ru3**) and $[Ru(phen)_2(1-Py-IQ)](PF_6)_2$ (**Ru4**)

N-Ts-phenethylamine and 2-pyridinecarboxaldehyde are dissolved in toluene, boron trifluoride etherate is added dropwise in an ice bath, refluxed at 60 °C under argon atmosphere, 30% NaOH, dehydrogenated at 120 °C to obtain 1-(2-pyridine Base)-isoquinoline. Reflowing 1-(2-pyridyl)-isoquinoline and *cis*- $[Ru(bpy)_2Cl_2] \cdot H_2O$  or *cis*- $[Ru(phen)_2Cl_2] \cdot H_2O$  in a solution of ethanol: water (1:1) overnight, and **Ru3** and **Ru4** were obtained finally.

Complex **Ru3** was a brown solid weigh 0.076 g, and its yield was 82%.  $^1H$  NMR (400 MHz, DMSO- $d_6$ )  $\delta$  8.99 (d,  $J = 8.3$  Hz, 1H), 8.96 – 8.90 (m, 1H), 8.90 – 8.79 (m,

4H), 8.24 – 8.09 (m, 6H), 8.12 – 7.93(m, 3H), 7.91 (dd, J = 5.7, 1.4 Hz, 1H), 7.88 – 7.79 (m, 2H), 7.78 – 7.68 (m, 2H), 7.65(d, J = 6.3 Hz, 1H), 7.56 (p, J = 7.1 Hz, 3H), 7.51 – 7.40 (m,2H). UV-Vis ( $\lambda/\text{nm}$ ,  $\epsilon/\text{M}^{-1}$ ) (PBS): 287(55250), 461(10150). ESI-MS (MeCN):  $m/z=309.91$  ( $[\text{M}-2\text{PF}_6]^{2+}$ ),  $m/z=764.70$  ( $[\text{M}-\text{PF}_6]^+$ ). Anal. calc. for  $\text{C}_{34}\text{H}_{26}\text{F}_{12}\text{N}_6\text{P}_2\text{Ru}$ : C, 44.89%; H, 2.88%; N, 9.24%; found: C, 44.91%; H, 2.87%; N, 9.21%.

Complex **Ru4** was a brown solid weigh 0.076 g, and its yield was 82%.  $^1\text{H}$  NMR (400 MHz,  $\text{DMSO}-d_6$ )  $\delta$  9.04 (d, J = 8.5 Hz, 1H), 8.97 (d, J = 8.4 Hz, 1H), 8.90 – 8.76 (m, 2H), 8.79 – 8.72 (m, 2H), 8.50 – 8.35 (m, 4H), 8.39 – 8.24 (m, 2H), 8.25 – 8.14 (m, 2H), 8.14 – 8.04 (m, 1H), 8.04 – 7.83 (m, 7H), 7.83 – 7.67 (m, 2H), 7.67 – 7.58 (m, 1H), 7.46 (ddd, J = 7.3, 5.6, 1.2 Hz, 1H). UV-Vis ( $\lambda/\text{nm}$ ,  $\epsilon/\text{M}^{-1}$ ) (PBS): 263(58600), 371(8650). ESI-MS (MeCN):  $m/z=334.05$  ( $[\text{M}-2\text{PF}_6]^{2+}$ ),  $m/z= 812.88$  ( $[\text{M}-\text{PF}_6]^+$ ). Anal. calc. for  $\text{C}_{38}\text{H}_{26}\text{F}_{12}\text{N}_6\text{P}_2\text{Ru}$ : C, 47.66%; H, 2.74%; N, 8.78%; found: C, 47.63%; H, 2.76%; N, 8.80%.

#### 4.3. Cell culture conditions and cytotoxicity assay in vitro

All cell lines were cultured in Roswell Park Memorial Institute 1640 culture media supplemented with 10% fetal bovine serum and incubated at 37 °C in a 5%  $\text{CO}_2$  incubator. The  $\text{IC}_{50}$  values in Table 1 were measured by MTT assay according to our previous report [66].

#### 4.4. Stability assay

Stability assay of the Ru(II) complexes were measured by UV/Vis spectroscopy and  $^1\text{H}$  NMR according to the literature method [45]. The complexes were firstly dissolved in DMSO and then diluted with PBS. The UV/Vis spectra were scanned every three hours in 12 h. For  $^1\text{H}$  NMR spectra studies, the Ru(II) complexes (10  $\mu\text{M}$ ) were stored in  $\text{DMSO}-d_6/\text{D}_2\text{O}$  (v/v, 3/1) at 37 °C for 7 days. The  $^1\text{H}$  NMR spectra were measured at different time intervals (0, 1, 3, 7 days). The stability of Ru (II) complexes in aqueous solutions containing bovine serum albumin was tested

according to previous report [83].

#### 4.5. *Log $P_{o/w}$ measurement*

Log  $P_{o/w}$  is the partition coefficient between octanol and water. It was determined by using the flask-shaking method as previously described [66, 84]. Briefly, a suitable volume of a stock solution of the Ru(II) complex in aqueous NaCl was added to an equal volume of octanol, and the mixture was shaken for 48 h at 200 rpm at 25 °C to allow partitioning. The aqueous layer was separated from the octanol layer after the sample was centrifuged at 3000 rpm for 10 min. The Ru(II) content in the aqueous layer was measured by ICP-MS (NEXION-300X, PerkinElmer, USA). Finally, Log  $P_{o/w}$  values were calculated according to the equation of  $\text{Log } P_{o/w} = \text{Log} ([\text{Ru}]_o/[\text{Ru}]_w)$ .

#### 4.6. *Cellular uptake and localization*

NCI-H460 cells were seeded into six-well plates ( $5.0 \times 10^5$  cells per well) and grown overnight at 37 °C in a 5% CO<sub>2</sub> incubator. The cells were incubated with the different concentrations (1, 2, 4 μM) of Ru(II) complexes for different time intervals (1, 3, 6 h). After the incubation, the cells were harvested and washed twice with PBS. Cell Mitochondria Isolation Kit was used to extract the nuclear, mitochondrial and cytoplasmic fractions of the NCI-H460 cells. The pellets were digested with 3 mL concentrated nitric acid and 1 mL perhydrol for 24 h, and then diluted to 5 mL with ultrapure water. Finally, ICP-MS was used to determine the amount of Ru(II) complexes uptaken by NCI-H460 cells.

#### 4.7. *The mechanism of cellular uptake studies*

First, NCI-H460 cells were pretreated with endocytosis inhibitors (10 mM of NaN<sub>3</sub>, 50 μM of DOG, 0.25 mM of Sucrose and 10 μg/mL of Nystatin) for 2 h or at 4 °C for 4 h, respectively, and then incubation with 4 μM **RuIQ-1** or **RuIQ-2** for 6 h. Second, the control sample was exposed to 4 μM of **RuIQ-1** or **RuIQ-2** at 37 °C for 6 h. Finally, the intracellular uptake of **RuIQ-1** or **RuIQ-2** was determined using

ICP-MS after the cells trypsinized and collected.

#### 4.8. Apoptosis analysis

First, incubated NCI-H460 cells with **RuIQ-1** and **RuIQ-2** respectively, the cell nuclei were stained with Hoechst 33342 (5  $\mu\text{g}/\text{mL}$ ), washed twice with PBS, and then photographed using an inverted fluorescence microscope (Nikon, Japan). Second, after incubation with different concentrations (1, 2, 4  $\mu\text{M}$ ) of **RuIQ-1** and **RuIQ-2** respectively, NCI-H460 cells were harvested and washed with PBS for two times and re-suspended in 500  $\mu\text{L}$  binding buffer. The suspension was stained with Annexin V-FITC (5  $\mu\text{L}$ ) and PI (10  $\mu\text{L}$ ) in the dark. Finally, the resulting fluorescence was detected using the flow cytometer (BECKMAN COULTER, USA).

#### 4.9. MMP measurement

The MMP was measured by using both inverted fluorescence microscope and flow cytometry. After pretreatment with different concentration (1, 2 and 4  $\mu\text{M}$ ) of **RuIQ-1** and **RuIQ-2** for different time (3, 6 and 12 h), the NCI-H460 cells were trypsinized and washed twice with PBS. For microscope observation, the collected cells were incubated in complete medium containing JC-1 (10  $\mu\text{g}/\text{mL}$ ) for 30 min and washed with PBS twice, and then imaged an inverted fluorescence microscope (Nikon, Japan). For flow cytometry analysis, the cells were trypsinized and washed twice with PBS, and then incubated in 500  $\mu\text{L}$  PBS containing JC-1 (10  $\mu\text{g}/\text{mL}$ ) for 30 min at 37  $^{\circ}\text{C}$ . The cells were analyzed by flow cytometer after trypsinized and washed twice with PBS.

#### 4.10. ROS assay

NCI-H460 cells seeded into six-well plates were incubated with the different concentration (1, 2 and 4  $\mu\text{M}$ ) of **RuIQ-1** and **RuIQ-2** for 12 h, then incubated with DCFH-DA (10  $\mu\text{M}$ ) in culture medium for 20 min at 37  $^{\circ}\text{C}$ . After treatment, the levels of intracellular ROS were analyzed by inverted fluorescence microscope and flow

cytometer. Besides, NCI-H460 cells were pretreated with NAC (10 mM) or GSH (5 mM) for 1 h and then treated with **RuIQ-2** (2  $\mu$ M) for 12 h before flow cytometer analysis.

#### 4.11. Comet assay

The DNA damage was investigated by single-cell gel electrophoresis [66], which was performed using the Comet assay reagent kit. DNA was stained with SYBR Green I (Trevigen) and imaged under an inverted fluorescence microscope.

#### 4.12. Cell cycle arrest analysis

The cell cycle distribution was investigated by flow cytometry analysis. Briefly, NCI-H460 cells were incubated with different concentrations (1, 2 and 4  $\mu$ M) of Ru(II) complexes for 24 h. After that, the collected cells were stained with PI (50  $\mu$ g/mL) in the presence of RNAase A (100  $\mu$ g/mL) for 30 min at 37 °C, and then analyzed using the flow cytometer.

#### 4.13. Western blot assay

The effects of complex **RuIQ-2** on expression levels of proteins associated with caspase, Bcl-2 family, cytochrome *c*, DNA damage and cell cycle were analyzed by western blot assay. The western blot assay was performed as previously described [46,59]. The protein bands were visualized using ChemiDoc<sup>TM</sup> XRS+ Imaging System (Bio-Rad, USA).

#### 4.14. The *in vivo* toxicity assay

The *in vivo* toxicity of complex **RuIQ-2** was assessed on developing zebrafish embryos. Zebrafish embryos were provided by the Zebrafish Platform of Affiliated hospital of Guangdong Medical University. Zebrafish embryos were incubated in 12-well plates with 2 mL embryo water containing different concentrations of **RuIQ-2** (0, 2, 4, 8, 16 and 32  $\mu$ M) at  $28.0 \pm 1.0^\circ\text{C}$ . Each group has 12 zebrafish

embryos. The development of zebrafish embryos was imaged under a DFC310 FX microscope (Leica Microsystems CMS GmbH, Germany) every 24 h. The ethical protocols used for the *in vivo* zebrafish embryo study were conducted in line with the ethics regulations of Guangdong Medical University.

All assays were performed at least three times, and all of the data were expressed as the mean  $\pm$  SD.

## Acknowledgements

This work was supported by the National Natural Science Foundation of China (No. 21701034, No.81773175 and No.11704343), Major Scientific Research Projects in Guangdong Province (Special Innovative Projects) (No. 2017KTSCX078, 2018KQNCX100), the China Postdoctoral Science Foundation (No. 2018M630839), the Natural Science Foundation of Guangdong Province (No.2020A1515010444), and the Public Service Platform of South China Sea for R&D Marine Biomedicine Resources, Marine Biomedical Research Institute, the Opening Project of Guangdong Province Key Laboratory of Computational Science at the Sun Yat-sen University (No. 2018017), and the University Student Innovation Experiment Program.

The authors are very grateful to Prof. Jingjing Zhang for providing Zebrafish Platform.

## Appendix A. Supplementary data

Supplementary data related to this article can be found at [Http://](http://)

## References

- [1] X. Li, K. Heimann, X.T. Dinh, F.R. Keene, J.G. Collins, Biological processing of dinuclear ruthenium complexes in eukaryotic cells, *Mol. Biosyst.* 12 (2016) 3032-3045.
- [2] D.G. Hottinger, D.S. Beebe, T. Kozhimannil, R.C. Prielipp, K.G. Belani, Sodium nitroprusside in 2014: A clinical concepts review, *Journal of anaesthesiology, Clin. Pharmacol.* 30 (2014) 462-471.
- [3] R.A. Haque, A.W. Salman, S. Budagumpi, A.A.-A. Abdullah, A.M.S.A. Majid, Sterically

tuned Ag(i)- and Pd(ii)-N-heterocyclic carbene complexes of imidazol-2-ylidenes: synthesis, crystal structures, and in vitro antibacterial and anticancer studies, *Metallomic*. 5 (2013) 760-769.

[4] R. Motterlini, B.E. Mann, R. Foresti, Therapeutic applications of carbon monoxide-releasing molecules, *Expert. Opin. Inv. Drug*. 14 (2005) 1305-1318.

[5] A.S. Bhagavathula, A.A. Elnour, A. Shehab, Alternatives to currently used antimalarial drugs: in search of a magic bullet, *Infect. Dis. Poverty*. 5 (2016) 103.

[6] H. Huang, B. Yu, P. Zhang, J. Huang, Y. Chen, G. Gasser, L. Ji, H. Chao, Highly Charged Ruthenium(II) Polypyridyl Complexes as Lysosome-Localized Photosensitizers for Two-Photon Photodynamic Therapy, *Angew. Chem. Int. Ed. Engl.* 54 (2015) 14049-14052.

[7] E. Păunescu, S. McArthur, M. Soudani, R. Scopelliti, P.J. Dyson, Nonsteroidal Anti-inflammatory—Organometallic Anticancer Compounds, *Inorg. Chem.* 55 (2016) 1788-1808.

[8] M. Li, L. Lai, Z. Zhao, T. Chen, Aquation Is a Crucial Activation Step for Anticancer Action of Ruthenium(II) Polypyridyl Complexes to Trigger Cancer Cell Apoptosis, *Chem. Asian. J.* 11 (2016) 310-320.

[9] Y. Zhou, Q. Yu, X. Qin, D. Bhavsar, L. Yang, Q. Chen, W. Zheng, L. Chen, J. Liu, Improving the Anticancer Efficacy of Laminin Receptor-Specific Therapeutic Ruthenium Nanoparticles (RuBB-Loaded EGCG-RuNPs) via ROS-Dependent Apoptosis in SMMC-7721 Cells, *ACS. Appl. Mater. Inter.* 8 (2016) 15000-15012.

[10] Z.P. Zeng, Q. Wu, F.Y. Sun, K.D. Zheng, W.J. Mei, Imaging Nuclei of MDA-MB-231 Breast Cancer Cells by Chiral Ruthenium(II) Complex Coordinated by

2-(4-Phenyacetylenophenyl)-1H-imidazo[4,5f][1,10]phenanthroline, *Inorg. Chem.* 55 (2016) 5710-5718.

[11] R.R. Ye, C.P. Tan, L.N. Ji, Z.W. Mao, Coumarin-appended phosphorescent cyclometalated iridium(iii) complexes as mitochondria-targeted theranostic anticancer agents, *Dalton Trans.* 45 (2016) 13042-13051.

[12] P.C.A. Bruijninx, P.J. Sadler, Controlling platinum, ruthenium, and osmium reactivity for anticancer drug design, in: R. van Eldik, C.D. Hubbard (Eds.) *Adv. Inorg. Chem.* 61 (2009) 1-62

[13] G. Palermo, A. Magistrato, T. Riedel, T. von Erlach, C.A. Davey, P.J. Dyson, U. Rothlisberger, Fighting Cancer with Transition Metal Complexes: From Naked DNA to Protein and Chromatin Targeting Strategies, *Chem. Med. Chem.* 11 (2016) 1199-1210.

[14] Z.H. Siddik, Cisplatin: mode of cytotoxic action and molecular basis of resistance, *Oncogene.* 22 (2003) 7265-7279.

[15] M.D. Hall, K.A. Telma, K.-E. Chang, T.D. Lee, J.P. Madigan, J.R. Lloyd, I.S. Goldlust, J.D. Hoeschele, M.M. Gottesman, Say No to DMSO: Dimethylsulfoxide Inactivates Cisplatin, Carboplatin, and Other Platinum Complexes, *Cancer Res.* 74 (2014) 3913-3922.

[16] M. Abid, F. Shamsi, A. Azam, Ruthenium Complexes: An Emerging Ground to the Development of Metallopharmaceuticals for Cancer Therapy, *Mini-Rev. Med. Chem.* 16 (2016) 772-786.

[17] P. Zhang, P.J. Sadler, Advances in the design of organometallic anticancer complexes, *J. Organomet. Chem.* 839 (2017) 5-14.

[18] K.D. Mjos, C. Orvig, Metallodrugs in Medicinal Inorganic Chemistry, *Chem. Rev.* 114

(2014) 4540-4563.

[19] A. Bergamo, G. Sava, Ruthenium anticancer compounds: myths and realities of the emerging metal-based drugs, *Dalton Trans.* 40 (2011) 7817-7810.

[20] Christian, G. Hartinger, Michael, A. Jakupec, S. Zorbas-Seifried, M. Groessler, A. Egger, W. Berger, H. Zorbas, Paul, J. Dyson, Bernhard, K. Keppler, KP1019, A New Redox-Active Anticancer Agent - Preclinical Development and Results of a Clinical Phase I Study in Tumor Patients, *Chem. Biodivers.* 5 (2010) 2140-2155.

[21] Petra, Heffeter, Katharina, Böck, Bihter, Atil, Mir, Ali, Reza, Hoda, Intracellular protein binding patterns of the anticancer ruthenium drugs KP1019 and KP1339, *J. Biol. Inorg. Chem.* 15 (2010) 737-48.

[22] S. Monro, K.L. Colón, H. Yin, J. Roque, P. Konda, S. Gujar, R.P. Thummel, L. Lilge, C.G. Cameron, S.A. McFarland, Transition Metal Complexes and Photodynamic Therapy from a Tumor-Centered Approach: Challenges, Opportunities, and Highlights from the Development of TLD1433, *Chem. Rev.* 119(2018) 797-828.

[23] E. Alessio, L. Messori, NAMI-A and KP1019/1339, Two Iconic Ruthenium Anticancer Drug Candidates Face-to-Face: A Case Story in Medicinal Inorganic Chemistry, *Molecules.* 24 (2019) 1995.

[24] J. Liu, H. Lai, Z. Xiong, B. Chen, T. Chen, Functionalization and cancer-targeting design of ruthenium complexes for precise cancer therapy, *Chem. Commun.* 55 (2019) 9904-9914.

[25] L. Zeng, Y. Chen, H. Huang, J. Wang, D. Zhao, L. Ji, H. Chao, Cyclometalated ruthenium (II) anthraquinone complexes exhibit strong anticancer activity in hypoxic tumor cells, *Chem-Euro.* 21 (2015) 15308-15319.

- [26] H. Huang, P. Zhang, B. Yu, Y. Chen, J. Wang, L. Ji, H. Chao, Targeting nucleus DNA with a cyclometalated dipyrrophenazineruthenium (II) complex, *J. Med. Chem.* 57 (2014) 8971-8983.
- [27] B. Peña, A. David, C. Pavani, M.S. Baptista, J.-P. Pellois, C. Turro, K.R. Dunbar, Cytotoxicity studies of cyclometallated ruthenium (II) compounds: New applications for ruthenium dyes, *Organometallics*. 33 (2014) 1100-1103.
- [28] V. Vidimar, C. Licon, R. Cerón-Camacho, E. Guerin, P. Coliat, A. Venkatasamy, M. Ali, D. Guenot, R. Le Lagadec, A.C. Jung, J.-N. Freund, M. Pfeffer, G. Mellitzer, G. Sava, C. Gaiddon, A redox ruthenium compound directly targets PHD2 and inhibits the HIF1 pathway to reduce tumor angiogenesis independently of p53, *Cancer. Lett.* 440-441 (2019) 145-155.
- [29] J.-B. Sortais, N. Pannetier, A. Holuigue, L. Barloy, C. Sirlin, M. Pfeffer, N. Kyritsakas, Cyclometalation of primary benzyl amines by Ruthenium (II), Rhodium (III), and Iridium (III) complexes, *Organometallics*. 26 (2007) 1856-1867.
- [30] L. Zeng, P. Gupta, Y. Chen, E. Wang, L. Ji, H. Chao, Z.-S. Chen, The development of anticancer ruthenium (II) complexes: from single molecule compounds to nanomaterials, *Chem. Soc. Rev.* 46 (2017) 5771-5804.
- [31] J.P. Djukic, J.B. Sortais, L. Barloy, M. Pfeffer, Cycloruthenated compounds—synthesis and applications, *Eur. J. Inorg. Chem.* 2009 (2009) 817-853.
- [32] B.A. Albani, B. Peña, K.R. Dunbar, C. Turro, New cyclometallated Ru (II) complex for potential application in photochemotherapy?, *Photoch. Photobio. Sci.* 13 (2014) 272-280.
- [33] J. Maksimoska, L. Feng, K. Harms, C. Yi, J. Kissil, R. Marmorstein, E. Meggers, Targeting large kinase active site with rigid, bulky octahedral ruthenium complexes, *J. Am. Chem.*

Soc.130 (2008) 15764-15765.

[34] M.A. Jakupec, M. Galanski, V.B. Arion, C.G. Hartinger, B.K. Keppler, Antitumour metal compounds: more than theme and variations, Dalton Trans. (2008) 183-194.

[35] T. Respondek, R.N. Garner, M.K. Herroon, I. Podgorski, C. Turro, J.J. Kodanko, Light activation of a cysteine protease inhibitor: caging of a peptidomimetic nitrile with Rull (bpy) 2, J. Am. Chem. Soc. 133 (2011) 17164-17167.

[36] V.M. Dembitsky, T.A. Glorizova, V.V. Poroikov, Naturally occurring plant isoquinoline N-oxide alkaloids: Their pharmacological and SAR activities, Phytomedicine. 22 (2015) 183-202.

[37] Y. Song, Z. Shao, T.S. Dexheimer, E.S. Scher, Y. Pommier, M. Cushman, Structure-based design, synthesis, and biological studies of new anticancer norindenoisoquinoline topoisomerase I inhibitors, J. Med. Chem. 53 (2010) 1979-1989.

[38] K.B. Huang, H.Y. Mo, Z.F. Chen, J.H. Wei, Y.C. Liu, H. Liang, Isoquinoline derivatives Zn (II)/Ni (II) complexes: crystal structures, cytotoxicity, and their action mechanism, Eur. J. Inorg. Chem. 100 (2015) 68-76.

[39] J. Dong, X.X. Shi, J.J. Yan, J. Xing, Q. Zhang, S. Xiao, Efficient and Practical One-Pot Conversions of N-Tosyltetrahydroisoquinolines into Isoquinolines and of N-Tosyltetrahydro- $\beta$ -carbolines into  $\beta$ -Carbolines through Tandem  $\beta$ -Elimination and Aromatization, Eur. J. Inorg. Chem. 2010 (2010) 6987-6992.

[40] B.P. Sullivan, D.J. Salmon, T.J. Meyer, Mixed Phosphine 2,2'-Bipyridine Complexes of Ruthenium, Inorg. Chem. 17 (1978) 3334-3341.

[41] J.P. Collin, J.P. Sauvage, Synthesis and study of mononuclear ruthenium(II) complexes of

sterically hindering diimine chelates. Implications for the catalytic oxidation of water to molecular oxygen, *Inorg. Chem.* 25 (1986) 135-141.

[42] J. Chen, F. Peng, Y. Zhang, B. Li, J. She, X. Jie, Z. Zou, M. Chen, L. Chen, *Synthesis*, characterization, cellular uptake and apoptosis-inducing properties of two highly cytotoxic cyclometalated ruthenium(II) beta-carboline complexes, *Eur. J. Med. Chem.* 140 (2017) 104-117.

[43] K.B. Huang, Z.F. Chen, Y.C. Liu, M. Wang, J.H. Wei, X.L. Xie, J.L. Zhang, K. Hu, H. Liang, Copper(II/I) complexes of 5-pyridin-2-yl-[1,3]dioxolo[4,5-g]isoquinoline: synthesis, crystal structure, antitumor activity and DNA interaction, *Eur. J. Med. Chem.* 70 (2013) 640-648.

[44] M.L. Muro-Small, J.E. Yarnell, C.E. McCusker, F.N. Castellano, *Spectroscopy and Photophysics in Cyclometalated Ru(II)-Bis(bipyridyl) Complexes*, *Eur. J. Inorg. Chem.* 2012 (2012) 4004-4011.

[45] Y. Zheng, L. He, D.-Y. Zhang, C.-P. Tan, L.-N. Ji, Z.-W. Mao, Mixed-ligand iridium(III) complexes as photodynamic anticancer agents, *Dalton Trans.* 46 (2017) 11395-11407.

[46] Y. Li, C.P. Tan, W. Zhang, L. He, L.N. Ji, Z.W. Mao, Phosphorescent iridium(III)-bis-N-heterocyclic carbene complexes as mitochondria-targeted theranostic and photodynamic anticancer agents, *Biomaterials.* 39 (2015) 95-104.

[47] K.K.W. Lo, B.T.N. Chan, H.W. Liu, K.Y. Zhang, S.P.Y. Li, T.S.M. Tang, Cyclometalated iridium(III) polypyridine dibenzocyclooctyne complexes as the first phosphorescent bioorthogonal probes, *Chem. Commun.* 49 (2013) 4271-4273.

[48] C. A. Puckett, J. K. Barton, Mechanism of Cellular Uptake of a Ruthenium Polypyridyl Complex, *Biochemistry.* 47(2008) 11711-11716.

- [49] C.A. Puckett, J.K. Barton, Methods to Explore Cellular Uptake of Ruthenium Complexes, *J. Am. Chem. Soc.* 129 (2007) 46-47.
- [50] H. Huang, P. Zhang, H. Chen, L. Ji, H. Chao, Comparison Between Polypyridyl and Cyclometalated Ruthenium(II) Complexes: Anticancer Activities Against 2D and 3D Cancer Models, *Chem-Euro.* 21 (2015) 715-725.
- [51] J. Chen, Y. Zhang, G. Li, F. Peng, X. Jie, J. She, G. Dongye, Z. Zou, S. Rong, L. Chen, Cytotoxicity in vitro, cellular uptake, localization and apoptotic mechanism studies induced by ruthenium(II) complex, *J. Biol. Inorg. Chem.* 23 (2018) 261-275.
- [52] I.M. Ghobrial, T.E. Witzig, A.A. Adjei, Targeting Apoptosis Pathways in Cancer Therapy, *CA - Cancer. J. Clin.* 55 (2005) 178-194.
- [53] T. Chen, Y.S. Wong, Selenocystine induces apoptosis of A375 human melanoma cells by activating ROS-mediated mitochondrial pathway and p53 phosphorylation, *Cell. Mol. Life. Sci.* 65 (2008) 2763-2775.
- [54] Z. Zhang, Q. Wu, X.H. Wu, F.Y. Sun, L.M. Chen, J.C. Chen, S.L. Yang, W.J. Mei, Ruthenium(II) complexes as apoptosis inducers by stabilizing c-myc G-quadruplex DNA, *Eur. J. Med. Chem.* 80 (2014) 316-324.
- [55] H. Lai, Z. Zhao, L. Li, W. Zheng, T. Chen, Antiangiogenic ruthenium (II) benzimidazole complexes, structure-based activation of distinct signaling pathways, *Metallomics.* 7 (2015) 439-447.
- [56] A. Takahashi, E.S. Alnemri, Y.A. Lazebnik, T. Fernandes-Alnemri, G. Litwack, R.D. Moir, R.D. Goldman, G.G. Poirier, S.H. Kaufmann, W.C. Earnshaw, Cleavage of lamin A by Mch2 alpha but not CPP32: multiple interleukin 1 beta-converting enzyme-related proteases with

distinct substrate recognition properties are active in apoptosis, *P. Natl. Acad. Sci. USA.* 93 (1996) 8395-8400.

[57] T. Chen, Y.S. Wong, Selenocystine induces caspase-independent apoptosis in MCF-7 human breast carcinoma cells with involvement of p53 phosphorylation and reactive oxygen species generation, *Int. J. Biochem. Cell. B.* 41 (2009) 666-676.

[58] L. Chen, G. Li, F. Peng, X. Jie, G. Dongye, K. Cai, R. Feng, B. Li, Q. Zeng, K. Lun, J. Chen, B. Xu, The induction of autophagy against mitochondria-mediated apoptosis in lung cancer cells by a ruthenium (II) imidazole complex, *Oncotarget.* 7 (2016) 80716-80734.

[59] S.H. Huang, L.W. Wu, A.C. Huang, C.C. Yu, J.C. Lien, Y.P. Huang, J.S. Yang, J.H. Yang, Y.P. Hsiao, W.G. Wood, C.S. Yu, J.G. Chung, Benzyl Isothiocyanate (BITC) Induces G2/M Phase Arrest and Apoptosis in Human Melanoma A375.S2 Cells through Reactive Oxygen Species (ROS) and both Mitochondria-Dependent and Death Receptor-Mediated Multiple Signaling Pathways, *J. Agr. Food. Chem.* 60 (2012) 665-675.

[60] H.U. Simon, A. Haj-Yehia, F. Levi-Schaffer, Role of reactive oxygen species (ROS) in apoptosis induction, *Apoptosis.* 5 (2000) 415-418.

[61] P.D. Ray, B.W. Huang, Y. Tsuji, Reactive oxygen species (ROS) homeostasis and redox regulation in cellular signaling, *Cell Signal.* 24 (2012) 981-990.

[62] C. Alapetite, Use of the alkaline comet assay to detect DNA repair deficiencies in human fibroblasts exposed to UVC, UVB, UVA and gamma-rays, *Int. J. Radiat. Biol.* 69 (1996) 359-369.

[63] W.P. Roos, B. Kaina, DNA damage-induced cell death by apoptosis, *Trends. Mol. Med.* 12 (2006) 440-450.

- [64] V. Romanov, T.C. Whyard, W.C. Waltzer, A.P. Grollman, T. Rosenquist, Aristolochic acid-induced apoptosis and G2 cell cycle arrest depends on ROS generation and MAP kinases activation, *Arch. Toxicol.* 89 (2015) 47-56.
- [65] C. Fan, J. Chen, Y. Wang, Y.-S. Wong, Y. Zhang, W. Zheng, W. Cao, T. Chen, Selenocystine potentiates cancer cell apoptosis induced by 5-fluorouracil by triggering reactive oxygen species-mediated DNA damage and inactivation of the ERK pathway, *Free. Radical Bio. Med.* 65 (2013) 305-316.
- [66] L. Chen, F. Peng, G. Li, X. Jie, K. Cai, C. Cai, Y. Zhong, H. Zeng, W. Li, Z. Zhang, The studies on the cytotoxicity in vitro, cellular uptake, cell cycle arrest and apoptosis-inducing properties of ruthenium methylimidazole complex [Ru (Melm) 4 (p-cpip)] 2+, *J. Inorg. Biochem.* 156 (2016) 64-74.
- [67] J. Chen, G. Li, F. Peng, X. Jie, G. Dongye, Y. Zhong, R. Feng, B. Li, J. Qu, Y. Ding, Investigation of inducing apoptosis in human lung cancer A549 cells and related mechanism of a ruthenium (II) polypyridyl complex, *Inorg. Chem. Commu.* 69 (2016) 35-39.
- [68] S.W. Lee, M.H. Lee, J.H. Park, S.H. Kang, H.M. Yoo, S.H. Ka, Y.M. Oh, Y.J. Jeon, C.H. Chung, SUMOylation of hnRNP-K is required for p53-mediated cell-cycle arrest in response to DNA damage, *Embo. J.* 31 (2012) 4441-4452.
- [69] C. Fan, J. Chen, Y. Wang, Y.S. Wong, Y. Zhang, W. Zheng, W. Cao, T. Chen, Selenocystine potentiates cancer cell apoptosis induced by 5-fluorouracil by triggering reactive oxygen species-mediated DNA damage and inactivation of the ERK pathway, *Free. Radic. Biol. Med.* 65 (2013) 305-316.
- [70] K.E. Erkkila, D.T. Odom, J.K. Barton, Recognition and reaction of metallointercalators with

- DNA, Chem. Rev. 99 (1999) 2777-2796.
- [71] C. Metcalfe, J.A. Thomas, Kinetically inert transition metal complexes that reversibly bind to DNA, Chem. Soc. Rev, 32 (2003) 215-224.
- [72] O. Seitz, DNA and RNA Binders. From Small Molecules to Drugs. Band 1 + 2. Herausgegeben von Martine Demeunynck, Christian Bailly und W. David Wilson, Angewandte Chemie. 115 (2003) 5143-5144.
- [73] A.M. Pyle, J.P. Rehmman, R. Meshoyrer, C.V. Kumar, N.J. Turro, J.K. Barton, Mixed-ligand complexes of ruthenium(II): factors governing binding to DNA, J. Am. Chem. Soc. 111 (1989) 3051-3058.
- [74] L.M. Chen, J. Liu, J.C. Chen, C.P. Tan, S. Shi, K.C. Zheng, L.N. Ji, Synthesis, characterization, DNA-binding and spectral properties of complexes  $[\text{Ru}(\text{L})_4(\text{dppz})]^{2+}$  (L=Im and Melm), J. Inorg. Biochem. 102 (2008) 330-341.
- [75] L.-M. Chen, J. Liu, J.-C. Chen, S. Shi, C.-P. Tan, K.-C. Zheng, L.-N. Ji, Experimental and theoretical studies on the DNA-binding and spectral properties of water-soluble complex  $[\text{Ru}(\text{Melm})_4(\text{dpq})]^{2+}$ , J. Mol. Struct. 881 (2008) 156-166.
- [76] J.K. Buolamwini, Cell cycle molecular targets in novel anticancer drug discovery, Curr. Pharm. Design. 6 (2000) 379-392.
- [77] R.M. Golsteyn, Cdk1 and Cdk2 complexes (cyclin dependent kinases) in apoptosis: a role beyond the cell cycle, Cancer. Lett. 217 (2005) 129-138.
- [78] M. Malumbres, M. Barbacid, Cell cycle, CDKs and cancer: a changing paradigm, Nat. Rev. Cancer. 9 (2009) 153.
- [79] V. Yadav, S. Sultana, J. Yadav, N. Saini, Gatifloxacin Induces S and G2-Phase Cell Cycle

Arrest in Pancreatic Cancer Cells via p21/p27/p53, Plos. One, 7 (2012) e47796.

[80] C. Zhang, C. Willett, T. Fremgen, Zebrafish: An Animal Model for Toxicological Studies, Curr. Pro. Toxic. 17 (2003) 1.7.1-1.7.18.

[81] L. Yang, N.Y. Ho, R. Alshut, J. Legradi, C. Weiss, M. Reischl, R. Mikut, U. Liebel, F. Müller, U. Strähle, Zebrafish embryos as models for embryotoxic and teratological effects of chemicals, Reprod.Toxicol. 28 (2009) 245-253.

[82] C. S. Anselmo, V.F. Sardela, V.P. Sousa, H.M.G. Pereira, Zebrafish (Danio rerio): A valuable tool for predicting the metabolism of xenobiotics in humans?, Comp. Biochem. Phys. C. 212 (2018) 34-46.

[83] M.H. Kaulage, B. Maji, S. Pasadi, S. Bhattacharya, K. Muniyappa, Novel ruthenium azo-quinoline complexes with enhanced photonuclease activity in human cancer cells, Eur. J. Inorg. Chem. 139 (2017) 1016-1029.

[84] H. Huang, P. Zhang, Y. Chen, K. Qiu, C. Jin, L. Ji, H. Chao, Synthesis, characterization and biological evaluation of labile intercalative ruthenium (II) complexes for anticancer drug screening, Dalton Trans. 45 (2016) 13135-13145.

### Research highlights

- Two new cyclometalated Ru(II) complexes were synthesized and characterized.
- **RuIQ-1** and **RuIQ-2** display higher activities than that of cisplatin against NCI-H460 cells.
- **RuIQ-2** exhibits low toxicity toward zebrafish embryos *in vivo*.
- The mitochondrial membrane potential, ROS and DNA damage were investigated.
- The cellular uptake, cell cycle arrest and apoptosis-inducing mechanism were explored.

**Declaration of interests**

The authors declare that they have no known competing financial interests or personal relationships that could have appeared to influence the work reported in this paper.

The authors declare the following financial interests/personal relationships which may be considered as potential competing interests: